The Role of direct Asphaltene Inhibitors on Asphaltene Stabilization during Gas Injection

[1]Asghar Gandomkar[*], [2]Hamid Reza Nasriani

[1] Department of Chemical and Petroleum Engineering, Faculty of Chemical and Material Engineering, Shiraz Branch, Islamic Azad University, Shiraz, Iran

[2]School of Engineering, Faculty of Science and Technology, University of Central Lancashire, Preston, PR1 2HE, United Kingdom

Abstract

There are a large number of investigations, which evaluate the impact of the liquid-based inhibitors on the asphaltene stabilization. In those studies, a specific volume of inhibitor was added to the oil sample and the asphaltene precipitation is then studied. However, this method is indirectly applicable to processes like gas injection. For that reason, in this work, the metal oxide nanoparticles (GO, TiO_2, SiO_2, and MgO) have been considered in the liquid-free mode as direct asphaltene inhibitors (DAIs) on asphaltene stabilization for the duration of miscible CO_2 injection. The dissolution of DAIs in CO_2 was investigated by measurement of cloud point pressure to evaluate the pressure/temperature conditions, need for certifying that the CO_2/DAIs mixtures have the single-phase condition. Afterwards, the impact of DAI was studied on asphaltene precipitation and deposition by static and dynamic approaches. Results show that the total size of asphaltene particles which precipitated during injection of miscible CO_2/DAIs mixture is significantly lower than that for immiscible pure CO_2 injection. The amount of asphaltene deposition significantly decreased during injection of miscible CO_2/DAIs mixtures compared to immiscible pure CO_2 injection. Additionally, the metal oxide nanoparticles hinder

[*] **Corresponding Author**
Email Addresses: agandomkar@shirazu.ac.ir (Asghar Gandomkar)

the phase separation of asphaltenes kinetically and prevent growth. It is conducted by stabilizing the colloidal suspension of the asphaltene particles, which are in sub-micrometre size to significantly slow the asphaltene flocculation onset.

Keywords: CO_2 Injection, Asphaltene Stabilization, Direct Asphaltene Inhibitors, Cloud Point Pressure, Metal Oxide Nanoparticles.

1. Introduction

The application of different substances, which efficiently stabilize or solubilize asphaltene in crude oils, is both preventive and remedial measures, additionally; it saves costs and eases its application during gas injection (Joonaki et al., 2019; Leonar et al., 2013; Stephenson, 1990). Asphaltene precipitation/deposition is encountered during gas injection due to changes in reservoir oil composition. The asphaltene deposition leads to reservoir wettability alteration, formation damage, plugging of the wellbore and downhole facilities, consequently, it will harm the project economics because of delays in production and expensive clean-up operations. The impact of chemical inhibitors on the asphaltene stabilization during CO_2 flooding has been investigated thoroughly. Several chemical products have been developed and investigated. The chemical inhibitors are mainly selected based on their efficiency, availability, and environmental impacts. The inhibitors are commonly categorized based on their molecular structures, chemical characteristic, functional groups, alkyl tails, and aromaticity factor (Yin et al., 2000). There are numerous studies in the literature which investigate the impact of liquid-based inhibitors on the asphaltene stabilization in crude oil samples (Hong et al., 2004; Kazemzadeh et al., 2015; Lu et al., 2016; Bae et al., 2016; Shojaati et al., 2017; Varamesh et at., 2019). For example, Rocha et al., (2006) studied a large number of asphaltene inhibitors, e.g. ethoxylated nonylphenols, organic acids, dodecylbenzene sulfonic acid (DBSA), salicylic acid, and vegetable oils. They

reported a significant solubilization effect by DBSA. This finding highlighted the significant impact of acid-base interactions. In addition, Hu et al., (2005) illustrated that nut oils have an acceptable effectivity in the inhibition processes. Besides, Taher et al., (2002) considered different chemicals as asphaltene inhibitors, i.e., DBSA, deasphalted crude oil (DO), resins (R), toluene (T), the nonylphenol (NP) and dodecyl risol sinol (DR). Consequently, the capability of the aforementioned chemicals on the inhibition of the asphaltene deposition was in this manner: DR > DBSA > NP > R > T > DO. Moreover, the combination of DO and T at 60 weight percent performed satisfactorily and the impact of NP and DBSA was analogous to DR. Joonaki et al., (2020) considered an asphaltenic oil mixed with a wax inhibitor-containing oil to investigate the interaction of asphaltenes and waxes using the quartz crystal microbalance technique. They showed that the different wax inhibitor chemistries illustrated different outcomes regarding the asphaltene deposition tendency and lead to change the pour point and oil viscosity. Reubush (1999) investigated some other chemicals as asphaltene inhibitors, the chemicals were as follow: carboxylic and sulfonic acids, ethoxylated alcohols, phenols, and amines. They concluded that ethoxylated alcohols and phenols are the best inhibitors. Hong et al., (2004) studied the impact of two inhibitors: an anionic surfactant (sodium dodecyl sulfate) and a cationic surfactant (cetylpyridinium chloride). It was evident that the combination of an alkane tail with acidic functional group improved the asphaltene inhibition performance. Kelland (2009) reported that nonylphenol (NP) has a decent inhibition capability on asphaltene aggregation; this is because the OH functional group and alkane tail with 9 carbons are attached to the benzene ring. If phenol and nonylphenol are compared, it highlights the effect of polar group and alkanes tail length in the inhibitor. In the literature, the liquid-based chemicals were generally utilized and were added to the crude oil or chemical solution that was injected into the reservoir. For

example, Ibrahim et al., (2004), Hassanpour et al., (2016 and 2018), and Varamesh et al., (2019) were added the CO_3O_4, toluene, TiO_2, and NiO/Fe_3O_4 nanoparticles as inhibitors, respectively, to the Saskatchewan and Asmari reservoir crude oils. Moreover, in the case of chemical solution flooding into the reservoir cores, Lu et al., (2016) inspected the impact of Al_2O_3 nanoparticles on the asphaltene deposition by conducting core flood experiments. The coreflooding results indicated that the Al_2O_3/nanofluid injection can hinder the asphaltene precipitation in porous medium and consequently the reservoir permeability does not decrease. In addition, the simultaneous injection of CO_2 and nano-fluid is more sufficient than the cyclic injection. Also, Karambeygi et al., (2016) indicated that the salicylic acid can inhibit the asphaltene precipitation. In addition, the high polar/aromatic inhibitors are similar to natural state of the resins which can keep asphaltene particles in solution. Joonaki et al., (2017) investigated the asphaltene precipitation using a quartz crystal microbalance technique to provide the most suitable scenario for injection of commercial inhibitors/solvent at field conditions. Their results illustrated that the reservoir conditions (pressure and temperature) and presence of gas might change the ranking of commercial inhibitors for reducing the asphaltene precipitation. Consequently, the conventional treatment of asphaltene precipitation/deposition is categorized into two methods during gas injection: (a) the liquid-based chemical was added to the crude oil samples as asphaltene inhibitors and (b) the gas alternating chemical solution (inhibitors) injection into the reservoir. The first case is not applicable in the field scale and just illustrates the performance of the inhibitor on asphaltene stabilization in crude oils. Also, the second scenario can be used in field-scale, but it involves three-phase flow. Three-phase displacement (oil, gas, and chemical solution) can be provided with some limitation during gas injection. The process is highly affected by gravity at higher gas mobility and the gas/chemical solution gravity segregation can

play a negative role in this process. However, in our previous work (Azizkhani and Gandomkar, 2020), liquid-free chemicals have been used as direct asphaltene inhibitors through CO_2 injection for the first time. This method involves two-phase flow displacement along with the inhibitor. Based on our previous work, the metal oxide nanoparticles (Fe_3O_4 and Al_2O_3) were considered as inhibitors while CO_2 injection. Subsequently, the asphaltene stabilization through CO_2/nanoparticles injection was investigated using static precipitation tests for two different live oil samples, i.e., volatile and intermediate live oil. Furthermore, it was noted that the amount of asphaltene precipitation was mitigated when CO_2/nanoparticles was injected compared to the case when pure CO_2 was injected. In addition, the mixtures that contain Fe_3O_4 could perform better than Al_2O_3 solutions; therefore the impact of solubility is more dominant than the effect of the aggregation during the injection of DAI. However, this study focused on asphaltene deposition in carbonate reservoir cores by analyses of dynamic asphaltene tests. Four metal oxide nanoparticles such as GO, TiO_2, SiO_2, and MgO were used as DAIs for asphaltene precipitation to make the asphaltene more stable in the insitu oil sample during the injection of the carbon dioxide. The cloud point pressure was monitored to ensure that the mixture of CO_2/nanoparticles is single-phase. Once the impact of DAIs was studied on asphaltene deposition at the reservoir conditions by static and dynamic asphaltene tests. This study considered a new approach for the application of inhibitors in porous media during gas injection. This method can be performed for other asphaltene inhibitors (alkaline and surfactant-based chemicals) as direct asphaltene inhibitors.

2. Materials and methods

- **Direct asphaltene inhibitors (DAI)**

Four metal oxide nanoparticles such as the graphene oxide (GO, MW = 12.01 gr/mol), titanium dioxide (TiO_2, MW = 79.87 gr/mol), silicon dioxide (SiO_2, MW = 60.08 gr/mol), and magnesium oxide (MgO, MW = 40.3 gr/mol) were used as direct inhibitor agents to make the asphaltene more stable in the reservoir live oil during the immiscible/miscible carbon dioxide injection. The metal oxide nano-particles generally have acidic, basic or amphoteric chemical characteristics, which causes polar interactions between asphaltenes molecules and nano-particles. However, the chemical nature of metal oxide nanoparticles considered in this study is acidic (SiO_2 and TiO_2) and basic (MgO and GO) (Nassar et al., 2011; Dai et al., 2014). All the inhibitors are commercially available and were used in the experiment as they were received. Different concentrations of nanoparticles were used in this study, i.e. 50, 100, 200, and 300 ppm for GO and 500, 1000, 2000, and 3000 ppm for other DAIs. The SARA (Saturates, Aromatics, Resins and Asphaltenes) analysis of reservoir crude oil with ^{o}API of 23.65 was reported in Table 1. The colloidal instability index (CII) was considered to investigate the instability of the crude oil. It should be noted that the CII is an index which highlights the ratio of asphaltene and saturate summation to the summation of resins and aromatics. If the CII value of a crude oil sample is greater than 0.9, the crude oil is expressed as unstable (Ghloum et al., 2010 and 2019). However, according to SARA data, the CII value for reservoir crude oils is 1.60, and it demonstrates the asphaltene precipitation possibilities for these cases. However, in this work, the recombined live oil was used in the experiments to study the asphaltene deposition at the reservoir conditions. The results of a constant composition expansion (CCE) experiment were used to guarantee that the recombined oil could represent the in-situ reservoir fluid with acceptable accuracy. The CCE result illustrates that the measured bubble point pressure is

consistent with the real reservoir oil bubble point pressure (Gandomkar et al., 2012). The reservoir pressure and temperature are 3150 psia and 60 ^{o}C, respectively.

Table 1

- **Cloud point pressure measurements**

The authors considered liquid-free additives as DAIs throughout CO_2 injection at the reservoir conditions. The dissolution of DAIs (GO, TiO_2, SiO_2, and MgO) in CO_2 was investigated by calculation of cloud point pressures. The cloud point appears the pressure at which cloudiness in the solution is first observed as the pressure is lowered. It was measured by HPHT visual cell with different concentrations based on our previous work (Azizkhani and Gandomkar, 2020). At first, a determined amount of DAI is weighed out and insert into the window cell. After that, a specified amount of CO_2 was added to the sample to provide the desired composition. The mixture with constant total composition was pressurized and then used a magnetic stirrer to create a rotating magnetic field (2000 rpm). It was continued to achieve single-phase solutions from the window cell at favorable temperatures and pressures. Finally, the reduction in pressure of all samples was considered at the intervals of 40 psi. The equilibrium condition took about two hours to identify any visual changes. Also more time might be needed for the low solubility materials. In general, the cloud point pressures of DAI/CO_2 were indicated in the fog form by visual monitoring in the bulk sample (Miller et al., 2009; Lee et al., 2016). The measurements were repeated at least three times with reproducibility of ±5 psi. Subsequently, these mixtures were considered in all experiments to certify that the single-phase solution has occurred.

- **Minimum miscibility pressure (MMP)**

The IFT measurements between the live oil and DAI/CO_2 were performed by the high-pressure high-temperature IFT 700 apparatus. All the mixtures of hydrocarbon gas and DAIs were provided and then used to measure the IFTs at reservoir conditions (i.e. 3150 psia and 60 ^{o}C). An oil droplet is produced from the end of the capillary needle, which surrounded by pure CO_2 or DAI/CO_2 at required conditions. However, the IFTs were measured using advanced drop shape analysis software. In addition, the IFT error calculated via the standard deviation of 4 repeated measurements of each mix, and it was about ± 0.1. Also, the MMP measurement was conducted using vanishing interfacial tension (VIT) procedure (Azizkhani and Gandomkar, 2020; Ghorbani et al., 2014).

- **Asphaltene precipitation, Static test**

To investigate the asphaltene precipitation throughout the injection of CO_2 and CO_2/DAI, the PVT analysis was conducted. The PVT apparatus that was used in this study consisted the followings: PVT cell, transfer container, back pressure regulation, air bath, HPLC pump, sampling vessel, filter, recombination cell, and shaker. In the experiment, a certain volume of the CO_2/DAI mixture was injected into the PVT cell that contained live oil at the reservoir conditions. Next, the PVT cell was shaken for 24 hours at a chosen temperature and pressure. Then, the mixture of the CO_2/DAI and live oil was then retained in a stationary position for another day to ensure that the asphaltene precipitation was occurring. The crude oil sampling is taken out for analysis of asphaltene precipitation during CO_2/DAI injection. High-pressure filtration was used to separate the precipitated asphaltene from the oil at a constant pressure during its displacement from the PVT cell into the sampling vessel. Subsequently, the IP 143 standard method was conducted to measure the amount of the asphaltene content of the sample for all CO_2/DAI mixtures (Azizkhani and Gandomkar, 2020; Arciniegas et al., 2014).

- **Asphaltene deposition, Dynamic test**

In order to study the impact of DAIs on the asphaltene precipitation and its deposition, a series of coreflooding experiments were conducted during immiscible/miscible injection of CO_2. Full details of the coreflooding process, the core flood apparatus and its components are provided elsewhere (Gandomkar et al., 2015). To understand the impact of DAIs on asphaltene precipitation and its subsequent deposition, the miscible CO_2/DAIs was injected into carbonate core samples with the initial water and oil saturations similar to those of the initial reservoir conditions. In the course of the core flood experiments, the produced oil was gathered to measure the asphaltene deposition into the carbonate cores. To accurately determine the asphaltene content in the produced oil using spectrophotometry, a minimum of one gram of produced oil sample was required (Nguele et al., 2016; Srivastava et al., 1999; Li et al., 2018). The CO_2 injection was conducted up to two pore volumes with a frontal advance rate of 0.1 cm^3/min. Also, the scaling criterion of Rappaport and Leas (1953) has been considered to remove the dependence of oil recovery factor on core length and gas injection rate due to capillary end effect. It should be noted that the amount of asphaltene deposition was estimated by subtraction of the asphaltene content of the original crude oil from that of the produced oil. The amount of asphaltene deposition divided by initial asphaltene content and has been reported as a dimensionless parameter. The properties of carbonate cores were reported in Table 2. The average porosity and permeability ranged between 13 to 16 percent and 7 to 9 md, respectively (Cao et al., 2013).

Table 2

3. Results and discussion

The effect of GO, TiO_2, SiO_2, and MgO, as direct asphaltene inhibitors, on asphaltene precipitation and deposition was studied during miscible CO_2 injection. The SARA analysis and CII values were conducted to show the asphaltene precipitation possibilities for these cases. Besides, the cloud point pressure of all the CO_2/nanoparticles mixtures was measured to ensure that the single-phase conditions have occurred during asphaltene precipitation tests. Also, the asphaltene precipitation and deposition investigated by static and dynamic tests, respectively at reservoir conditions (i.e. 60 ^oC and 3150 psia).

- **Phase behavior of DAI/CO_2 by cloud point pressure measurements**

In Table 3, the cloud point pressures of CO_2 mixtures with GO, TiO_2, SiO_2, and MgO for different temperatures of 25, 40, 60, and 80 ^oC is listed. It should be noted that, throughout cloud point pressure measurements, the concentration of nano-particles were ranging from 50 to 300 ppm for GO and 500 to 3000 ppm for others. The cloud point pressures were ranging from 1400 to nearly 2500 psia. The cloud point pressure normally rises as the concentration of nano-particles in the solution increases. Additionally, the cloud point pressures increase almost linearly with increase in temperature. e.g., the cloud point pressures of GO illustrated that the dissolution of direct asphaltene inhibitor in CO_2 has occurred at 1712, 1830, 1994, and 2159 psia in different concentration; 50, 100, 200, and 300 ppm; respectively at reservoir temperature (i.e. 60 ^oC). According to these observations, all the cloud point pressures are lower than reservoir pressure and consequently, the single-phase conditions occur during asphaltene precipitation/deposition tests for all direct asphaltene inhibitors. The effect of temperature on the cloud point pressure of CO_2/DAI is shown in Figure 1 at different concentrations. Additionally, the solubility of DAIs increase as the temperature decreases. This observation highlights that the

density is directly proportional to the solubility. It could be explained by the entropy of mixing and its dependency to the temperature. The density of CO_2 reduces significantly at higher temperatures, whereas the impact of temperature on the nanoparticles density is minimal. If the density of CO_2 becomes significantly different from that of nanoparticles, the entropy of mixing becomes negative and then the temperature has a converse impact on the system (Joung et al., 2002). Based on these results, the cloud point pressures of GO are lower than other nanoparticles considered in this study at the same temperature. The molecular weights of nanoparticles have an impact on the solubility in CO_2, this is due to entropic impacts and coupled with the unwanted enthalpy interactions related to the CO_2-phobic functionalities and CO_2 (Yu et al., 2014; Chu et al., 2019). As it was observed, all the DAIs/CO_2 mixtures were single-phase at reservoir conditions and then these solutions were used for all asphaltene precipitation experiments.

Table 3

Figure 1

- **MMP measurements**

The amount of asphaltene precipitation will be different during miscible and immiscible CO_2 injection. Cao et al., (2013) illustrated that the miscible CO_2 injection causes more asphaltene precipitation compared to immiscible injection. However, in this study, vanishing interfacial tension technique was used to investigate the effect of DAI on MMP. At first, at equilibrium pressures ranging from 2500 to 3150 psia, the interfacial tension between live oil and pure/DAIs CO_2 were assessed. It should be noted that all the IFT values were measured at the reservoir temperature and pressures higher than the cloud point pressure to make sure that the mixtures of the CO_2/Nanoparticles are single phase. In Table 4, the results of live oil-pure CO_2 and

DAIs/CO_2 mixtures at T_{res}= 60 ^{o}C are listed. Considering the data of Table 4, the IFT for pure CO_2, 200 ppm GO, 2000 ppm TiO_2, 2000 ppm SiO_2, and 2000 ppm MgO are 46, 13, 15, 14, and 15 dyne/cm, respectively at 2500 psia and 60 ^{o}C. The asphaltenes are known to be one of the most surface-active compounds in crude oil and could be absorbed to the DAIs surface and reduce the IFTs. The metal oxide (DAIs) surface will typically have high surface energy. It was noted that GO could expressively decrease IFT compared to other DAIs considered in this study. It referred to the high specific surface area of GO compared to other DAIs. In addition, an increase in equilibrium pressure led to a significant reduction in IFT. It is well understood that as the IFT between live oil and nanoparticles/carbon dioxide decreases it will increase the miscibility and subsequently leads to a decrease in the residual oil saturation (Ghorbani et al., 2014). As shown in Figure 2, it is noted that MMP decreases as the concentration of the nanoparticles increases. It is due to the fact that the density of the mixture of the nanoparticles and CO_2 is slightly larger than the pure carbon-dioxide; this leads to a lower difference in density with that of the live oil and therefore smaller IFT values than pure carbon-dioxide (Chu et al., 2019). It is also shown that the MMP for GO/CO_2 is lower than that of the other mixtures. The MMPs are 3370, 2941, 3006, 2938, and 3040 psia for pure CO_2, 200 ppm GO, 2000 ppm TiO_2, 2000 ppm SiO_2, and 2000 ppm MgO, respectively at reservoir temperature, 60 ^{o}C. Hence, the MMP for pure CO_2 is above the P_{res}=3150 psi; and consequently, the immiscible conditions will occur during pure CO_2 injection for asphaltene precipitation/deposition tests. Furthermore, the MMPs for all CO_2/DAIs are smaller than reservoir pressure, and as a result, miscible conditions occur during static and dynamic asphaltene processes.

Table 4

Figure 2

- **PVT analysis of asphaltene precipitation through CO_2/DAI injection**

In this work, the team used nanoparticles as direct asphaltene inhibition agent to prevent the asphaltene precipitation by static test during CO_2 injection. In all experiments, to guarantee that all solutions are single-phase, the mixtures of CO_2/nanoparticles were injected at a pressure higher than the cloud point pressure. The live oil has 6.4 weight percent initial asphaltene content and from Table 5, the amounts of 5.8 weight percent asphaltene precipitated during pure immiscible injection of CO_2. It was expected that the amount of asphaltene precipitation increases during miscible DAIs/CO_2 but it reduced using nanoparticles as direct asphaltene inhibitors. The amount of asphaltene precipitation reduced from 5.8 to 3.1, 4.2, 4, and 3.8 weight percent by using 100 ppm GO, 1000 ppm TiO_2, 1000 SiO_2, and 1000 ppm MgO mixtures, respectively. Additionally, the CO_2/GO mixtures decreased the amounts of asphaltene precipitation higher than other DAIs considered in this study. The specific surface area of the GO (890 m^2/g) is higher than that for TiO_2 (174.5 m^2/g), SiO_2 (590 m^2/g), and MgO (300 m^2/g); consequently, it led to more adsorption of asphaltene (Yu et al., 2014; Karambeygi et al., 2016; Chu et al., 2019). The application of nanoparticles could enhance the solubility of asphaltene in the live oil and consequently lead to a reduction in the precipitation of asphaltene. Likewise, it increases the CO_2 solubility, dilutes the live oil, subsequently disperses the resin molecules, and finally leads to asphaltene stabilization in oil. Also, the amounts of asphaltene precipitation decreased by increasing DAI concentrations. The lone pair electrons, i.e., a pair of valence electrons, of oxygen intensify the surface negative charge density of the metal oxide nanoparticles, which enhances the adsorption of asphaltene fraction. It should be noted that there is an insignificant reduction in asphaltene precipitation for the duration of a high concentration of DAIs. For example, the amounts of asphaltene precipitation are 2.5 and 2.4 weight percent for

200 and 300 ppm GO, respectively. For that reason, the DAI concentration of 200 ppm can be more efficient than other DAI concentrations through miscible CO_2/GO injection. It was previously reported that the optimal concentration for Fe_3O_4 and TiO_2 nanoparticles in the inhibitor is approximately one weight percent (Hassanpour et al., 2018). In addition, it will decrease the asphaltene precipitation to seventeen and eighteen percent of initial content of asphaltene using TiO_2 and Fe_3O_4 correspondingly. When a low concentration of inhibitor is applied, active site on the structure of asphaltene could be occupied by free monomers and consequently stabilizes the asphaltene particles within the solution (Rocha et al., 2006). Additionally, the polar head group of the inhibitor has a dissimilar potential to attach to the particles and makes the system of the inhibitor/asphaltene more stable. It should be highlighted that these groups' polarity governs the strength of the bond. However, when a high concentration of inhibitors is used, it will not lead to the desired result. As the inhibitors' concentration rises, the likelihood of self-association under hydrogenous bonding increases accordingly. Conversely, when a higher concentration of inhibitor is applied, the potential of self-association in inhibitor-inhibitor is larger than the inhibitor/asphaltene's interaction. Consequently, the capability of inhibitors on the stabilization of the asphaltenes decreases and it will cause the inhibitors to underperform at higher concentrations (Karambeygi, 2016; Leon et al., 2001). As a result, the metal oxide nanoparticles have acidic/basic/amphoteric chemical characteristic, which causes polar interactions between asphaltenes particles and nanoparticles. The bond formation between nanoparticles (metal oxide) and asphaltene particles is a key factor that delays the beginning point of separation of asphaltenes from oil, i.e., onset. The asphaltene particles could be suspended in resins due to the formation bonding of metal-oxide nanoparticles and asphaltene molecules and its bonding to the activated sites on the surface of the asphaltene particles (Nassar

et al., 2011). It should be noted there are two conflicting forces affecting the precipitation, i.e., aggregation effect and the solubility mechanism. The first force (aggregation effect) has a tendency to lead to precipitation whilst the second (solubility mechanism) tends to retain the asphaltene molecules in the solution. Furthermore, the results show that the impact of the solubility mechanism is more dominant than that of the aggregation effect for the duration of the injection of CO_2/nanoparticles (Gharbi et al., 2017; Rashid et al., 2019; Yen et al., 2001).

Table 5

- **The effect of DAI on asphaltene deposition**

The amount of asphaltene deposition into the carbonate cores was measured during coreflooding tests for pure and CO_2/DAIs injection. Figure 3 shows the variation in the asphaltene content of the produced oil with injected PV of pure and CO_2/DAIs injection during carbonate cores. The asphaltene concentration in the oil was constant till CO_2 breakthrough which occurred at around 0.25 pore volumes (PV) and 0.35 PV for pure CO_2 and CO_2/DAIs mixtures, respectively. Because the produced oil had not yet been in contact with the injected pure CO_2 and CO_2/DAIs, the change in asphaltene content was insignificant. Inversely, the asphaltene content in the produced oil after the CO_2 breakthrough reduced significantly. The drop in asphaltene content highlights the fact that some further asphaltene precipitation/flocculation occurs in the carbonate cores during pure and CO_2/DAIs injection. From Figure 3, the asphaltene content in produced oil during injection of DAIs/CO_2 mixtures are higher than that for pure CO_2 injection. It shows that the metal oxide nanoparticles can stabilize the asphaltene particles in reservoir oil. In addition, the mixture of GO/CO_2 improved the asphaltene stabilization compared to other DAIs considered in this study. From this result, the amount of asphaltene content in produced oil are 1.3, 5.4, 4.1, 3, and 5 weight percent after injection of 2 PV pure CO_2, 200 ppm GO, 2000 ppm

SiO_2, 2000 TiO_2, and 2000 ppm MgO mixtures, respectively. Also, Figure 4 illustrates the amount of asphaltene's deposition in the carbonate cores by the subtraction of the asphaltene content in the produced oil from that of the initial crude oil during the dynamic tests. The amount of asphaltene deposition significantly decreased during injection of CO_2/DAIs mixtures compared to pure CO_2 injection. The metal oxide nanoparticles hinder the phase separation of asphaltenes kinetically and prevent growth. It is conducted by stabilizing the colloidal suspension of the asphaltene particles, which are in sub-micrometer size to significantly slow the asphaltene flocculation onset. Consequently, the direct asphaltene inhibitors can prevent to asphaltene deposition and act as asphaltene dispersants. The polyaromatic nuclei with aliphatic side chains and rings of asphaltene connect and create micellar aggregates. This is well-documented that in addition to aromatic compounds, asphaltenes consist of different acidic and basic functional groups. The metal oxide nanoparticles that are adsorbed on the micelle core make the asphaltene micelles more stable. The DAIs connects to the asphaltene particles using their polar head and expands their aliphatic group outward. This creates a layer round asphaltenes. On the condition that the asphaltene particles are stabilized in the micelles, precipitation does not occur (Setaro rt al., 2019).

Figure 3

Figure 4

Besides, using asphaltene particle size analysis approach, the team measured the mean size of the asphaltene particles to study the impact of direct asphaltene inhibitors on asphaltene particle size for the duration of pure CO_2 injection and 200 ppm GO/CO_2 mixture injection, Figures 5 and 6. Based on this result, the asphaltene particle size during pure CO_2 injection is higher than that for GO/CO_2 mixture injection. It is clear that the GO/CO_2 mixtures can stabilize the asphaltene

particles in oil and significantly reduces the size of asphaltene particles simultaneously. The total size of asphaltene particles which precipitated during the injection of pure CO_2 and 200 ppm GO/CO_2 mixture are 2657808 and 756592 μm^2, respectively. The particles are created in two different stages, i.e., phase separation stage and asphaltene particle growth stage. Phase separation takes place when asphaltene particles in the oil precipitate and develop into large aggregates. Additionally, the stability of asphaltene particles can be improved by the introduction of compounds, which hold a polar head containing an acidic group, which can attach to the micellar core. Dissimilar acidities are observed for amphiphiles with diverse head groups. The inhibition capability of amphiphiles depends on the fact that how strong are their groups' acidity, therefore the amphiphiles stabilize the asphaltene in the solution via the acid-base interaction. The ability of amphiphiles' inhibition is related to the strength of these groups acidity and illustrating that the asphaltene stabilization occurs through the acid-base interaction (Zanganeh et al., 2018). However, direct asphaltene inhibitors can decrease the amount of asphaltene precipitation and also prevents the aggregation of precipitated asphaltene particles. By the way, the size of deposited asphaltene particles can affect the oil flow in porous media due to changing the pressure drop. Based on the dynamic tests, the differential pressure during the pure CO_2 injection was higher than that for injection of CO_2/DAIs mixtures. It referred to asphaltene precipitation, which increased formation damage during the pure CO_2 injection compared to other cases. Figure 7 shows the schematic of asphaltene deposition on the rock surface. The asphaltenes may adsorb onto the rock surface and cause permeability blockage, wettability alteration to oil-wet, reduces the oil effective permeability; and thereby decreases the oil recovery (Figure 7a). However, the application of direct asphaltene inhibitors can stabilize the asphaltene particles and also prevent to asphaltene deposition as a dispersant (Figure 7b).

Additionally, the presence of the metal oxide nanoparticles as direct asphaltene inhibitors can enhance the oil recovery factor between 6 to 25 percent compared to pure CO_2 injection. The adsorption performance of asphaltenes on the metal oxide nanoparticles is governed by two properties, i.e., the surface energy and the structure of nanoparticles and the chemical and physical characteristics of the asphaltene particles and polar, electrostatic, and van der Waals interactions are the key factors which influence the asphaltene adsorption onto the solid surfaces. Among these three factors, the acid−base (polar) and electrostatic interaction are the most significant factors. It is well-documented that surface Gibbs energy reduced by the adsorption of asphaltene particles on the nanoparticles. Consequently, the nanoparticles containing asphaltene (which are adsorbed onto the surface of nanoparticles) have a weaker interaction compared to those of the nanoparticles lacking asphaltene particles. Hence, the adsorbed asphaltene particles onto the nanoparticles have higher stability in the reservoir rock (Hosseinpour et al., 2013; Castro et al., 2009). Throughout the CO_2/DAIs injection, the nanoparticles adsorb the precipitated asphaltene particles and consequently alleviate the rate of the adsorption of precipitated asphaltenes onto the rock surface and consequent deposition in the porous medium. For that reason, the nanoparticles carrying asphaltenes could travel within the porous medium and subsequently lead to inhibit the precipitation and as a result, prevents permeability reduction due to asphaltene precipitation.

Figure 5

Figure 6

Figure 7

4. Conclusions

- Liquid-free inhibitors can be directly applicable for gas-based enhanced oil recovery in field scale.
- The metal oxide nanoparticles could increase the stability of the colloidal asphaltenes and consequently diminish the growing and the formation of flocculated asphaltene particles.
- The total size of asphaltene particles, which precipitated during injection CO_2/DAIs mixture, is significantly lower than that for pure CO_2 injection.
- The effectiveness of the graphene oxide nanoparticle is much better than other DAIs in retaining the asphaltene particles suspended and spread within the oil.
- The application of CO_2/GO mixtures could reduce the asphaltene aggregation/deposition and improved the oil recovery factor between 6 to 25 percent compared to the case that only CO_2 was injected.
- The cloud point pressure of CO_2/DAIs mixtures is under the reservoir pressure to certify that the single-phase solution has occurred at reservoir conditions.
- The direct asphaltene inhibitors lead to a decrease in the IFT and provide the miscible injection of gas at reservoir pressure and temperature.
- The metal oxide nanoparticles improved the solubility of the asphaltene particles and consequently kept them in the solution.

Nomenclature

Colloidal Instability Index, CII

Constant Composition Expansion, CCE

Cubic Plus Association Equation of state, CPA

Deasphalted Crude Oil, DO

Direct Asphaltene Inhibitor, DAI

Dodecyl Benzene Sulfonic Acid, DDBSA

Dodecyl Risolsinol, DR

Graphene Oxide, GO

High-Pressure High-Temperature, HPHT

Liquefied Petroleum Gas, LPG

Magnesium Oxide, MgO

Minimum Miscibility Pressure, MMP

Nonyl Phenol, NP

Pressure, Volume, Temperature, PVT

Resins, R

Saturates, Aromatics, Resins, and Asphaltenes, SARA

Silicon Dioxide, SiO_2

Titanium Dioxide, TiO_2

Toluene, T

Vanishing Interfacial Tension, VIT

Weight percent, wt

References

Arciniegas, L.M., Babadagli, T., Asphaltene precipitation, flocculation and deposition during solvent injection at elevated temperatures for heavy oil recovery, Fuel Journal, 124, 202-211, 2014.

Azizkhani A., Gandomkar, A., A novel method for application of nanoparticles as direct asphaltene inhibitors during miscible CO_2 injection, Journal of Petroleum Science and Engineering, 185, 106661, 2020.

Bae, J., Fouchard, D., Garner, S., Macias, J., Advantages of Applying a Multifaceted Approach to Asphaltene Inhibitor Selection, OTC 27171, 2016.

Cao, M., Gu, Y., Oil recovery mechanisms and asphaltene precipitation phenomenon in immiscible and miscible CO_2 flooding processes, Fuel Journal, 109, 157-166, 2013.

Castro, M., Cruz, J.L., Ramirez, S., Villegas, A., Predicting adsorption isotherms of asphaltenes in porous materials, Fluid Phase Equilibria, 286, 113-119, 2009.

Chu, T.M., Nguyen, N.T., Vu, T.L., Pham, T.D., Synthesis, Characterization, and Modification of Alumina Nanoparticles for Cationic Dye Removal, Materials, 12, 450, 1-15, 2019.

Dai, J.F., Wang, G.J., Wu, Ch., Investigation of the Surface Properties of Graphene Oxide and Graphene by Inverse Gas Chromatography, Chromatographia journal, 77, 299-307, 2014.

Gandomkar, A., Kharrat, R., Tertiary FAWAG Process on Gas and Water Invaded Zones, an Experimental Study, Journal of Energy Sources, Part A: Recovery, Utilization, and Environmental Effects, 34, 1913-1922, 2012.

Gandomkar, A., Rahimpour, M.R., Investigation of low salinity waterflooding in secondary and tertiary enhanced oil recovery in limestone reservoirs, Energy & Fuels Journal, 29, 7781-7792, 2015.

Gharbi, Kh., Benyounes, Kh., Khodja, M., Removal and prevention of asphaltene deposition during oil production: A literature review, Journal of Petroleum Science and Engineering, 158, 351-360, 2017.

Ghloum, E.F., Qahtani, M.A., Rashid, A., Effect of inhibitors on asphaltene precipitation for Marrat Kuwaiti reservoirs, Journal of Petroleum Science and Engineering, 70, 99-106, 2010.

Ghloum, E.F., Rashed, A.M., Safa, M.A., Mitigation of asphaltenes precipitation phenomenon via chemical inhibitors, Journal of Petroleum Science and Engineering, 175, 495-507, 2019.

Ghorbani, M., Momeni, ., Safavi, S., Gandomkar, A., Modified Vanishing Interfacial Tension (VIT) Test for CO_2-Oil Minimum Miscibility Pressure (MMP) Measurement, Journal of Natural Gas Science and Engineering, 20, 92-98, 2014.

Hassanpour, S., Malayeri, M.R., Riazi, M., Utilization of CO_3O_4 nanoparticles for reducing precipitation of asphaltene during CO_2 injection, Journal of Natural Gas Science and Engineering, 31, 39-47, 2016.

Hassanpour, S., Malayeri, M.R., Riazi, M., Asphaltene Precipitation during Injection of CO_2 Gas into a Synthetic Oil in the Presence of Fe_3O_4 and TiO_2 Nanoparticles, Journal of chemical engineering data, 63 (5), 1266-1274, 2018.

Hong, E., Watkinson, P., A study of asphaltene solubility and precipitation. Fuel journal, 83, 1881-1887, 2004.

Hosseinpour, N., Khodadadi, A.A., Bahramian, A., Mortazavi, Y., Asphaltene adsorption onto acidic/basic metal oxide nanoparticles toward in situ upgrading of reservoir oils by nanotechnology, Langmuir, 29, 14135-14146, 2013.

Hu, Y.F., Guo, T.M., Effect of the structures of ionic liquids and alkylbenzenederived amphiphiles on the inhibition of asphaltene precipitation from CO_2-injected reservoir oils, Langmuir, 21, 8168-8174, 2005.

Ibrahim, H.H., Idem, R.O., Inter relationships between Asphaltene Precipitation Inhibitor Effectiveness, Asphaltenes Characteristics, and Precipitation Behavior during n-Heptane (Light Paraffin Hydrocarbon) -Induced Asphaltene Precipitation, Energy & Fuels, 18, 1038-1048, 2004.

Joonaki, E., Burgass, R., Hassanpouryouzband, A., Tohidi, B., Comparison of experimental techniques for evaluation of chemistries against asphaltene aggregation and deposition: new application of high-pressure and high-temperature quartz, Energy & Fuels, 32, 3, 2712-2721, 2017.

Joonaki, E., Buckman, J., Burgass, R., Tohidi, B., Water versus Asphaltenes; Liquid–Liquid and Solid–Liquid Molecular Interactions Unravel the Mechanisms behind an Improved Oil Recovery Methodology, Scientific Reports, 9, 1, 11369, 2019.

Joonaki, E., Hassanpouryouzband, A., Burgass, R., Hase, A., Tohidi, B., Effects of Waxes and the Related Chemicals on Asphaltene Aggregation and Deposition Phenomena: Experimental and Modeling Studies, ACS omega 5, 13, 7124-7134, 2020.

Joung, S.N., Park, J.U., Kim, S.Y., High-pressure phase behavior of polymersolvent systems with addition of supercritical CO_2 at temperatures from 323.15 K to 503.15 K, Journal of Chemical & Engineering Data, 47, 2, 270-273, 2002.

Karambeygi, M.A., Nikazar, M., Kharrat, R., Experimental evaluation of asphaltene inhibitors selection for standard and reservoir conditions, Journal of Petroleum Science and Engineering, 13, 74-86, 2016.

Kazemzadeh, Y., Malayeri, M.R., Riazi, M., Parsaei, R., Impact of Fe_3O_4 nanoparticles on asphaltene precipitation during CO_2 injection, Journal of Natural Gas Science and Engineering, 22, 227-234, 2015.

Kelland, M.A., Asphaltene control. Production Chemicals for the Oil and Gas Industry. Stavanger, Norway: University of Stavanger, Chapter 4, 2009.

Leonard, G.Ch., Ponnapati, R., Rivers, G., Novel Asphaltene Inhibitor for Direct Application to Reservoir, SPE 167294, 2013.

Leon, O., Contreras, E., Rogel, E., Dambakli, G., Espidel, J., Aevedo, S., The influence of the adsorption of amphiphiles and resins in controlling asphaltene flocculation, Energy and Fuels, 15, 102-1032, 2001.

Lee, J.J., Dhuwe, A., Stephen, D., Eric, J., Enick, R.M., Polymeric and Small Molecule Thickeners for CO_2, Ethane, Propane and Butane for Improved Mobility Control, SPE Improved Oil Recovery Conference, Tulsa, SPE 179587, 2016.

Li, X., Guo, Y., Sun, Q., Lan, W., Guo, X., Experimental study for the impacts of flow rate and concentration of asphaltene precipitant on dynamic asphaltene deposition in microcapillary medium, Journal of Petroleum Science and Engineering, 162, 333-340, 2018.

Lu, T., Li, Zh., Fan, W., Zhang, X., Nanoparticles for Inhibition of Asphaltenes Deposition during CO_2 Flooding, Industrial & Engineering Chemistry Research, 55 (23), 6723-6733, 2016.

Miller, M.B., Chen, D.L., Xie, H.B., Luebke, D.R., Enick, R.M., Solubility of CO_2 in CO_2-philic oligomers; cosmotherm predictions and experimental results, fluid phase equilibria, 287, 26-32, 2009.

Nassar, N.N., Hassan, A., Pereira, A.P., Metal oxide nanoparticles for asphaltene adsorption and oxidation, Energy & Fuels, 25, 3, 1017-1023, 2011.

Nguele, R., Ghulami, M.R., Sasaki, K., Asphaltene Aggregation in Crude Oils during Supercritical Gas Injection, Energy and Fuels, 30, 2, 1266-1278, 2016.

Rappaport, L.A., Leas, W.J. 1953," Properties of Linear Waterfloods, presented at the Fall Meeting of the Petroleum Branch in Houston, Texas, SPE 213-G.

Rashid, Z., Wilfred, C.D., Murugesan, Th., A comprehensive review on the recent advances on the petroleum asphaltene aggregation, Journal of Petroleum Science and Engineering, 176, 249-268, 2019.

Reubush, S. D., Effects of storage on the linear viscoelastic response of polymer-modified asphalt at intermediate to high temperatures, MS Thesis, Virginia Polytechnic Institute and State University, Blacksburg, VA, 1999.

Rocha, L.C., Ferreira, M.S., Ramos, A.C., Inhibition of asphaltene precipitation in Brazilian crude oils using new oil soluble amphiphiles, Journal of Petroleum Science and Engineering, 51, 26-36, 2006.

Setaro, L.O., Pereira, V.J., Costa, G.M., Melo, S., A novel method to predict the risk of asphaltene precipitation due to CO_2 displacement in oil reservoirs, Journal of Petroleum Science and Engineering, 176, 1008-1017, 2019.

Shojaati, F., Riazi, M., Mousavi, S.H., Experimental investigation of the inhibitory behavior of metal oxides nanoparticles on asphaltene precipitation, Colloids and Surfaces A: Physicochemical and Engineering Aspects, 531, 99-110, 2017.

Srivastava, R.K., Huang, S.S., Dong, M., Asphaltene Deposition During CO_2 Flooding, SPE Production & Facilities, SPE 59092, 14, 4, 1999.

Stephenson, W.K., Producing Asphaltene Crude Oils: Problems and Solutions, Petroleum Engineer, 24, 1990.

Taher, A.S., Mohammed, A.F., Amal, S.E., Retardation of asphaltene precipitation by addition of toluene, resins, deasphalted oil and surfactants, Fluid Phase Equilibria 194-197, 1045-1057, 2002.

Varamesh, A., Hosseinpour, N., Prediction of Asphaltene Precipitation in Reservoir Model Oils in the Presence of Fe3O4 and NiO Nanoparticles by Cubic Plus Association Equation of State, Industrial & Engineering Chemistry Research, 58 (10), 4293-4302, 2019.

Yen, A., Yin, Y.R., Asomaning, S., Evaluating Asphaltene Inhibitors: Laboratory Tests and Field Studies, SPE 65376, 2001.

Yin, Y.R., Yen, A.T., Asphaltene Deposition and Chemical Control in CO_2 Floods, SPE-59293, 2000.

Yu, H., Li, Y., Fan, L., Yang, Sh., Highly dispersible and charge-tunable magnetic Fe_3O_4 nanoparticles: facile fabrication and reversible binding to GO for efficient removal of dye pollutants, Journal of Materials Chemistry A, 38, 2, 15763-15767, 2014.

Zanganeh, P., Dashti, .H, Ayatollahi, Sh., Comparing the effects of CH_4, CO_2, and N_2 injection on asphaltene precipitation and deposition at reservoir condition: A visual and modeling study, Fuel, 217, 633-641, 2018.

List of Tables

Table 1

Reservoir oil properties	Values
Saturates	55.10 wt
Aromatics	22.90 wt
Resins	15.60 wt
Asphaltenes	6.40 wt
CII	1.60
API	23.65
Molecular weight, g/mol, IP-86	164.80
S.G (60°F), ASTM-D40452	0.91
Acid Number, mg/g (KOH)	1.45
T_{res} (^{o}C)	60
P_{res} (psia)	3150

Table 2

Limestone Cores No.	Length (cm)	Diameter (in)	PV (cc)	Helium Porosity (Percent)	Permeability (mD)	Connate Water (Percent)
C1	7.5	1.5	11.9	13.91	7.5	27.9
C2	7.4	1.5	12.5	14.81	8.2	29.5
C3	7.7	1.5	13.3	15.15	8.6	28.4
C4	7.8	1.5	13.0	14.61	7.8	29.1
C5	7.7	1.5	13.1	14.92	8.3	28.5

Table 3

DAI	Concentration (ppm)	Cloud point pressure (psia)			
		25 °C	40 °C	60 °C	80 °C
GO	50	1419	1538	1712	1935
	100	1527	1659	1830	2061
	200	1670	1812	1994	2215
	300	1746	1971	2159	2406
TiO_2	500	1631	1724	1921	2126
	1000	1731	1862	2026	2243
	2000	1865	2028	2183	2388
	3000	1953	2159	2340	2589
SiO_2	500	1574	1663	1859	2080
	1000	1653	1725	1938	2180
	2000	1785	1947	2105	2300
	3000	1883	2082	2265	2497
MgO	500	1469	1575	1755	1971
	1000	1579	1690	1884	2118
	2000	1720	1882	2058	2263
	3000	1792	2046	2217	2483

Table 4

DAI	Concentration (ppm)	IFT (dyn/cm) Live oil/CO_2-DAI, T_{res}= 60 ^oC				
		P=2500 psia	P=2800 psia	P=3000 psia	P_{res} =3150 psia	MMP (psia)
GO	Pure CO_2	46	31	20	12	3370
	50	28	16	7	0	3100
	100	18	9	1	0	3049
	200	13	4	0	0	2941
	300	6	0	0	0	2740
TiO_2	500	34	19	8	0	3140
	1000	22	11	3	0	3115
	2000	15	6	1	0	3006
	3000	9	1	0	0	2811
SiO_2	500	31	16	5	0	3115
	1000	20	10	1	0	3027
	2000	14	4	0	0	2938
	3000	7	0	0	0	2761
MgO	500	30	19	8	0	3110
	1000	19	11	2	0	3100
	2000	15	7	0	0	3040
	3000	8	1	0	0	2814

Table 5

DAI	**Concentration (ppm)**	**Asphaltene Precipitation, Static Test** (wt%)
Pure CO_2		5.8
GO	50	4.0
	100	3.1
	200	2.5
	300	2.4
TiO_2	500	5.0
	1000	4.2
	2000	3.8
	3000	3.7
SiO_2	500	4.8
	1000	4.0
	2000	3.5
	3000	3.4
MgO	500	4.5
	1000	3.8
	2000	3.5
	3000	3.5

List of Figures

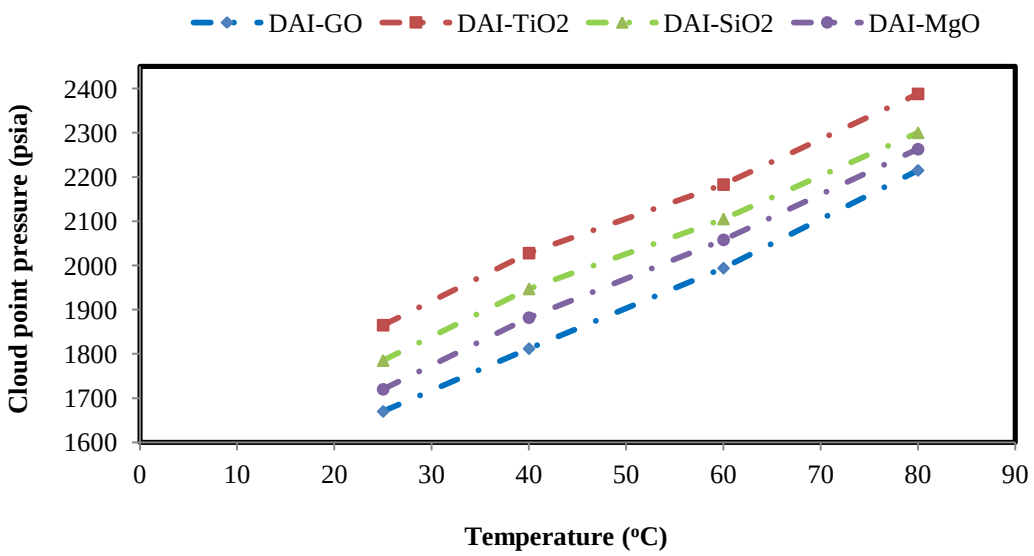
DAI-GO
DAI-TiO2
DAI-SiO2
DAI-MgO
Cloud point pressure (psia)
2400
2300
2200
2100
2000
1900
1800
1700
1600
0
10
20
30
40
50
60
70
80
90
Temperature (°C)

Figure 1

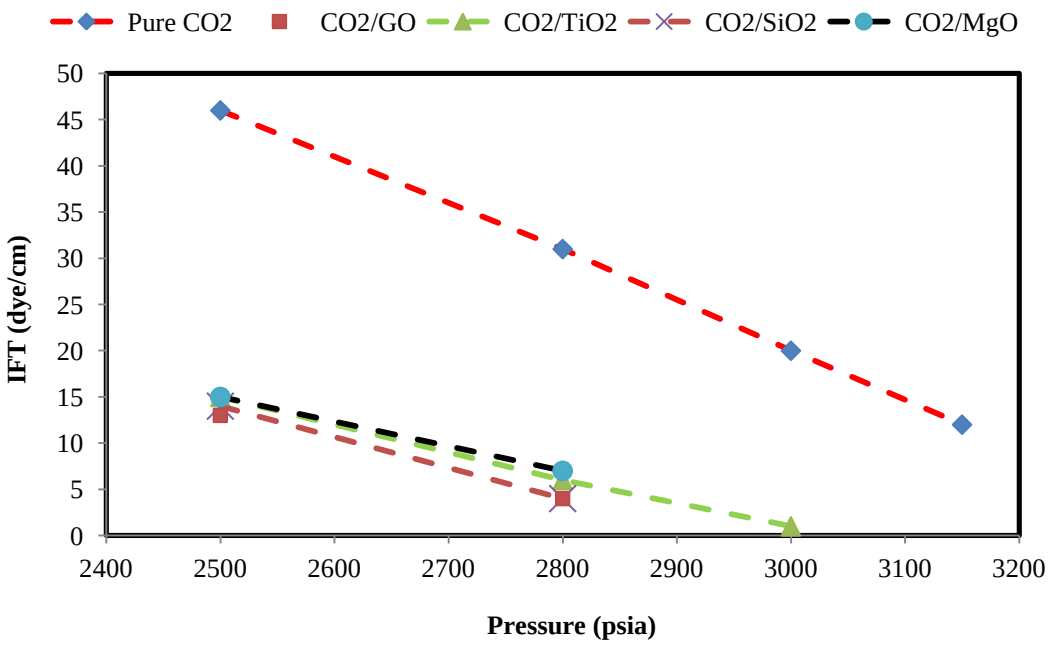
Pure CO2
CO2/GO
CO2/TiO2
CO2/SiO2
CO2/MgO
IFT (dye/cm)
Pressure (psia)
0
5
10
15
20
25
30
35
40
45
50
2400
2500
2600
2700
2800
2900
3000
3100
3200

Figure 2

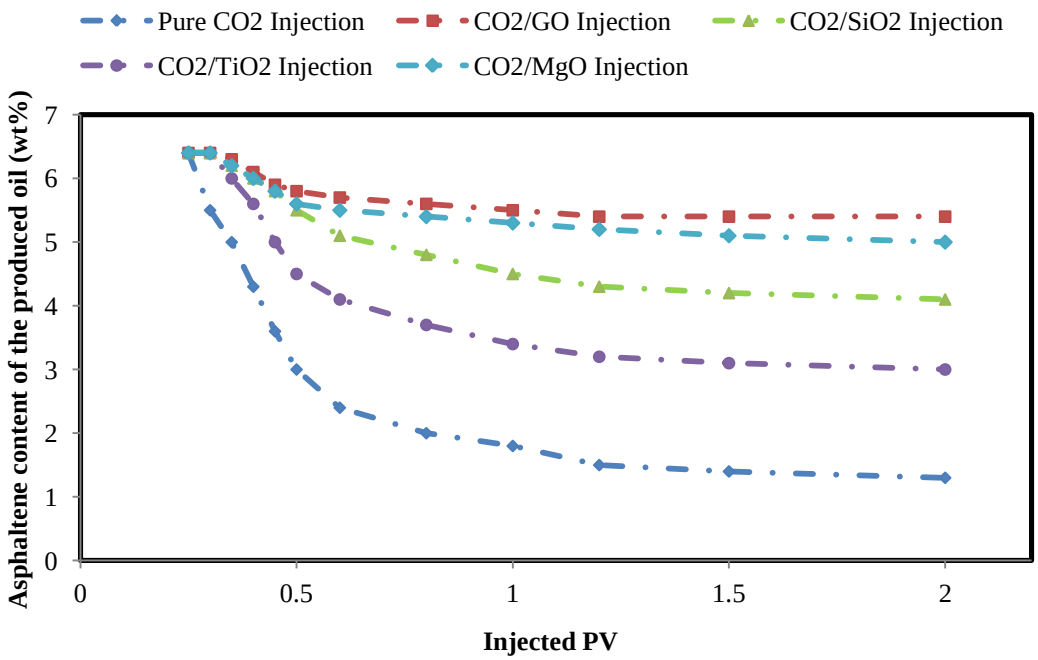
Pure CO2 Injection
CO2/GO Injection
CO2/SiO2 Injection
CO2/TiO2 Injection
CO2/MgO Injection
Asphaltene content of the produced oil (wt%)
0
1
2
3
4
5
6
7
0
0.5
1
1.5
2
Injected PV

Figure 3

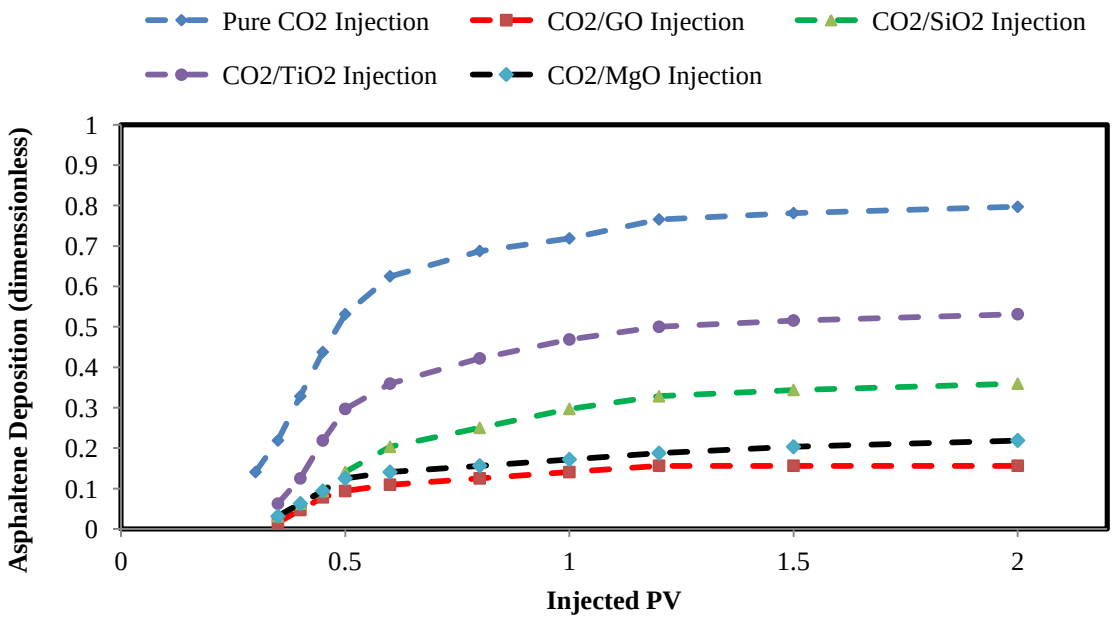
Pure CO2 Injection
CO2/GO Injection
CO2/SiO2 Injection
CO2/TiO2 Injection
CO2/MgO Injection
Asphaltene Deposition (dimenssionless)
Injected PV
0
0.1
0.2
0.3
0.4
0.5
0.6
0.7
0.8
0.9
1
0
0.5
1
1.5
2

Figure 4

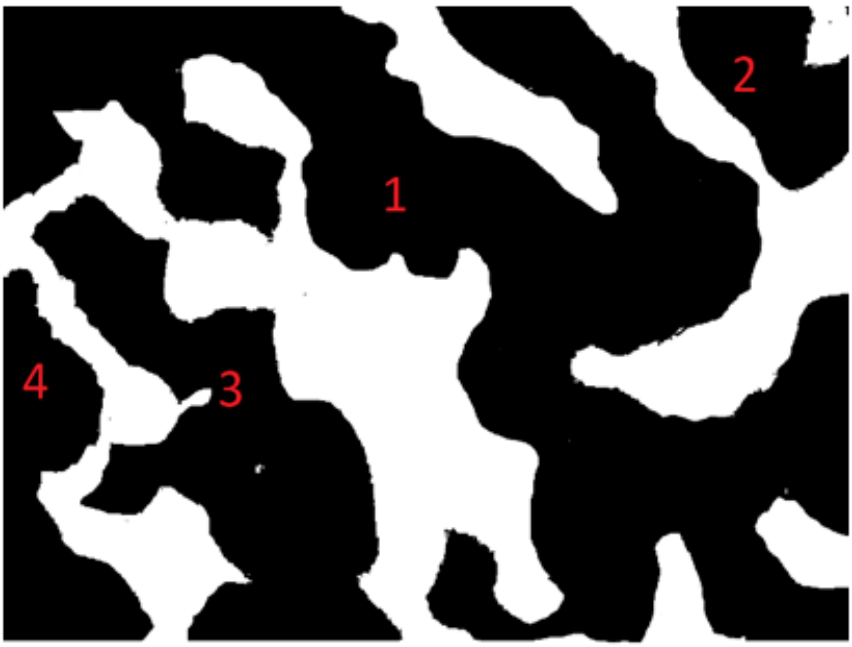

Particle number	1	2	3	4
Area (μm²)	1741670	157860	534393	223885
Total area (μm²)	2657808			

Figure 5

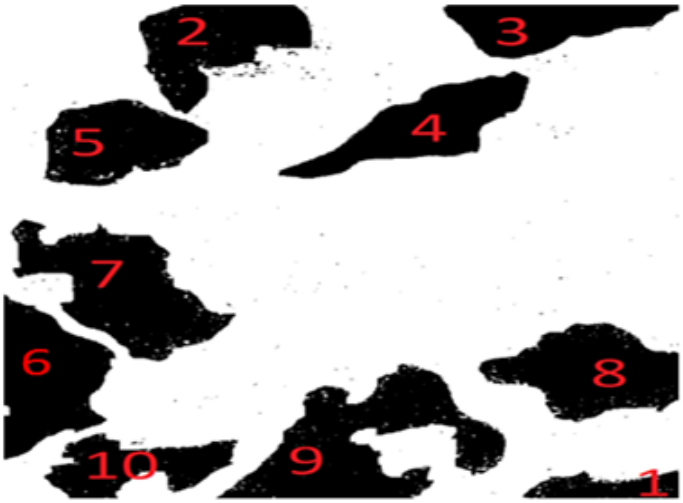

Particle number	1	2	3	4	5	6	7	8	9	10
Area (μm²)	29798	74005	53573	73264	68014	102846	104938	75591	125733	48830
Total area (μm²)	756592									

Figure 6

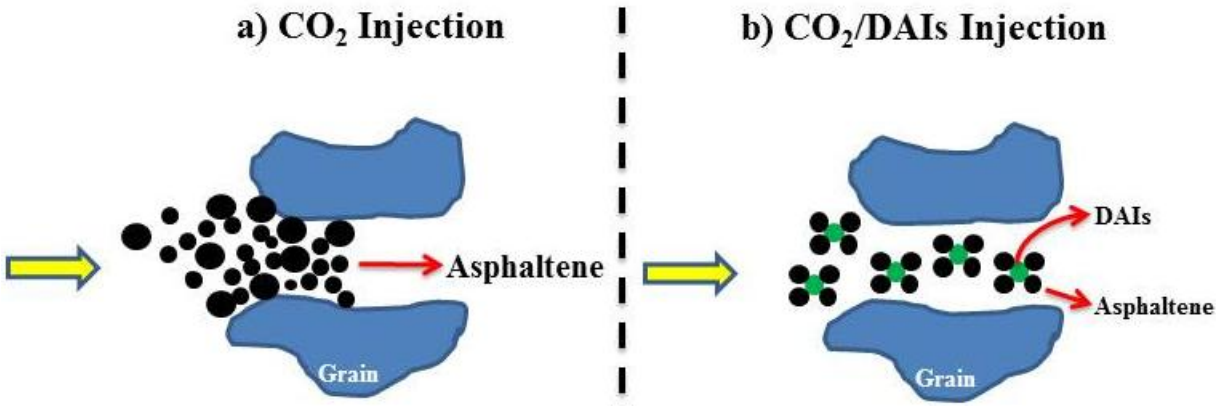
a) CO_2 Injection
b) CO_2/DAIs Injection
Asphaltene
Grain
DAIs
Asphaltene
Grain

Figure 7

The Role of direct Asphaltene Inhibitors on Asphaltene Stabilization during Gas Injection

[1]Asghar Gandomkar[*], [2]Hamid Reza Nasriani

[1] Department of Chemical and Petroleum Engineering, Faculty of Chemical and Material Engineering, Shiraz Branch, Islamic Azad University, Shiraz, Iran

[2]School of Engineering, Faculty of Science and Technology, University of Central Lancashire, Preston, PR1 2HE, United Kingdom

Abstract

There are a large number of investigations, which evaluate the impact of the liquid-based inhibitors on the asphaltene stabilization. In those studies, a specific volume of inhibitor was added to the oil sample and the asphaltene precipitation is then studied. However, this method is indirectly applicable to processes like gas injection. For that reason, in this work, the metal oxide nanoparticles (GO, TiO_2, SiO_2, and MgO) have been considered in the liquid-free mode as direct asphaltene inhibitors (DAIs) on asphaltene stabilization for the duration of miscible CO_2 injection. The dissolution of DAIs in CO_2 was investigated by measurement of cloud point pressure to evaluate the pressure/temperature conditions, need for certifying that the CO_2/DAIs mixtures have the single-phase condition. Afterwards, the impact of DAI was studied on asphaltene precipitation and deposition by static and dynamic approaches. Results show that the total size of asphaltene particles which precipitated during injection of miscible CO_2/DAIs mixture is significantly lower than that for immiscible pure CO_2 injection. The amount of asphaltene deposition significantly decreased during injection of miscible CO_2/DAIs mixtures compared to immiscible pure CO_2 injection. Additionally, the metal oxide nanoparticles hinder

[*] **Corresponding Author**
Email Addresses: agandomkar@shirazu.ac.ir (Asghar Gandomkar)

the phase separation of asphaltenes kinetically and prevent growth. It is conducted by stabilizing the colloidal suspension of the asphaltene particles, which are in sub-micrometre size to significantly slow the asphaltene flocculation onset.

Keywords: CO_2 Injection, Asphaltene Stabilization, Direct Asphaltene Inhibitors, Cloud Point Pressure, Metal Oxide Nanoparticles.

1. Introduction

The application of different substances, which efficiently stabilize or solubilize asphaltene in crude oils, is both preventive and remedial measures, additionally; it saves costs and eases its application during gas injection (Joonaki et al., 2019; Leonar et al., 2013; Stephenson, 1990). Asphaltene precipitation/deposition is encountered during gas injection due to changes in reservoir oil composition. The asphaltene deposition leads to reservoir wettability alteration, formation damage, plugging of the wellbore and downhole facilities, consequently, it will harm the project economics because of delays in production and expensive clean-up operations. The impact of chemical inhibitors on the asphaltene stabilization during CO_2 flooding has been investigated thoroughly. Several chemical products have been developed and investigated. The chemical inhibitors are mainly selected based on their efficiency, availability, and environmental impacts. The inhibitors are commonly categorized based on their molecular structures, chemical characteristic, functional groups, alkyl tails, and aromaticity factor (Yin et al., 2000). There are numerous studies in the literature which investigate the impact of liquid-based inhibitors on the asphaltene stabilization in crude oil samples (Hong et al., 2004; Kazemzadeh et al., 2015; Lu et al., 2016; Bae et al., 2016; Shojaati et al., 2017; Varamesh et at., 2019). For example, Rocha et al., (2006) studied a large number of asphaltene inhibitors, e.g. ethoxylated nonylphenols, organic acids, dodecylbenzene sulfonic acid (DBSA), salicylic acid, and vegetable oils. They

reported a significant solubilization effect by DBSA. This finding highlighted the significant impact of acid-base interactions. In addition, Hu et al., (2005) illustrated that nut oils have an acceptable effectivity in the inhibition processes. Besides, Taher et al., (2002) considered different chemicals as asphaltene inhibitors, i.e., DBSA, deasphalted crude oil (DO), resins (R), toluene (T), the nonylphenol (NP) and dodecyl risol sinol (DR). Consequently, the capability of the aforementioned chemicals on the inhibition of the asphaltene deposition was in this manner: DR > DBSA > NP > R > T > DO. Moreover, the combination of DO and T at 60 weight percent performed satisfactorily and the impact of NP and DBSA was analogous to DR. Joonaki et al., (2020) considered an asphaltenic oil mixed with a wax inhibitor-containing oil to investigate the interaction of asphaltenes and waxes using the quartz crystal microbalance technique. They showed that the different wax inhibitor chemistries illustrated different outcomes regarding the asphaltene deposition tendency and lead to change the pour point and oil viscosity. Reubush (1999) investigated some other chemicals as asphaltene inhibitors, the chemicals were as follow: carboxylic and sulfonic acids, ethoxylated alcohols, phenols, and amines. They concluded that ethoxylated alcohols and phenols are the best inhibitors. Hong et al., (2004) studied the impact of two inhibitors: an anionic surfactant (sodium dodecyl sulfate) and a cationic surfactant (cetylpyridinium chloride). It was evident that the combination of an alkane tail with acidic functional group improved the asphaltene inhibition performance. Kelland (2009) reported that nonylphenol (NP) has a decent inhibition capability on asphaltene aggregation; this is because the OH functional group and alkane tail with 9 carbons are attached to the benzene ring. If phenol and nonylphenol are compared, it highlights the effect of polar group and alkanes tail length in the inhibitor. In the literature, the liquid-based chemicals were generally utilized and were added to the crude oil or chemical solution that was injected into the reservoir. For

example, Ibrahim et al., (2004), Hassanpour et al., (2016 and 2018), and Varamesh et al., (2019) were added the CO_3O_4, toluene, TiO_2, and NiO/Fe_3O_4 nanoparticles as inhibitors, respectively, to the Saskatchewan and Asmari reservoir crude oils. Moreover, in the case of chemical solution flooding into the reservoir cores, Lu et al., (2016) inspected the impact of Al_2O_3 nanoparticles on the asphaltene deposition by conducting core flood experiments. The coreflooding results indicated that the Al_2O_3/nanofluid injection can hinder the asphaltene precipitation in porous medium and consequently the reservoir permeability does not decrease. In addition, the simultaneous injection of CO_2 and nano-fluid is more sufficient than the cyclic injection. Also, Karambeygi et al., (2016) indicated that the salicylic acid can inhibit the asphaltene precipitation. In addition, the high polar/aromatic inhibitors are similar to natural state of the resins which can keep asphaltene particles in solution. Joonaki et al., (2017) investigated the asphaltene precipitation using a quartz crystal microbalance technique to provide the most suitable scenario for injection of commercial inhibitors/solvent at field conditions. Their results illustrated that the reservoir conditions (pressure and temperature) and presence of gas might change the ranking of commercial inhibitors for reducing the asphaltene precipitation. Consequently, the conventional treatment of asphaltene precipitation/deposition is categorized into two methods during gas injection: (a) the liquid-based chemical was added to the crude oil samples as asphaltene inhibitors and (b) the gas alternating chemical solution (inhibitors) injection into the reservoir. The first case is not applicable in the field scale and just illustrates the performance of the inhibitor on asphaltene stabilization in crude oils. Also, the second scenario can be used in field-scale, but it involves three-phase flow. Three-phase displacement (oil, gas, and chemical solution) can be provided with some limitation during gas injection. The process is highly affected by gravity at higher gas mobility and the gas/chemical solution gravity segregation can

play a negative role in this process. However, in our previous work (Azizkhani and Gandomkar, 2020), liquid-free chemicals have been used as direct asphaltene inhibitors through CO_2 injection for the first time. This method involves two-phase flow displacement along with the inhibitor. Based on our previous work, the metal oxide nanoparticles (Fe_3O_4 and Al_2O_3) were considered as inhibitors while CO_2 injection. Subsequently, the asphaltene stabilization through CO_2/nanoparticles injection was investigated using static precipitation tests for two different live oil samples, i.e., volatile and intermediate live oil. Furthermore, it was noted that the amount of asphaltene precipitation was mitigated when CO_2/nanoparticles was injected compared to the case when pure CO_2 was injected. In addition, the mixtures that contain Fe_3O_4 could perform better than Al_2O_3 solutions; therefore the impact of solubility is more dominant than the effect of the aggregation during the injection of DAI. However, this study focused on asphaltene deposition in carbonate reservoir cores by analyses of dynamic asphaltene tests. Four metal oxide nanoparticles such as GO, TiO_2, SiO_2, and MgO were used as DAIs for asphaltene precipitation to make the asphaltene more stable in the insitu oil sample during the injection of the carbon dioxide. The cloud point pressure was monitored to ensure that the mixture of CO_2/nanoparticles is single-phase. Once the impact of DAIs was studied on asphaltene deposition at the reservoir conditions by static and dynamic asphaltene tests. This study considered a new approach for the application of inhibitors in porous media during gas injection. This method can be performed for other asphaltene inhibitors (alkaline and surfactant-based chemicals) as direct asphaltene inhibitors.

2. Materials and methods

- **Direct asphaltene inhibitors (DAI)**

Four metal oxide nanoparticles such as the graphene oxide (GO, MW = 12.01 gr/mol), titanium dioxide (TiO_2, MW = 79.87 gr/mol), silicon dioxide (SiO_2, MW = 60.08 gr/mol), and magnesium oxide (MgO, MW = 40.3 gr/mol) were used as direct inhibitor agents to make the asphaltene more stable in the reservoir live oil during the immiscible/miscible carbon dioxide injection. The metal oxide nano-particles generally have acidic, basic or amphoteric chemical characteristics, which causes polar interactions between asphaltenes molecules and nano-particles. However, the chemical nature of metal oxide nanoparticles considered in this study is acidic (SiO_2 and TiO_2) and basic (MgO and GO) (Nassar et al., 2011; Dai et al., 2014). All the inhibitors are commercially available and were used in the experiment as they were received. Different concentrations of nanoparticles were used in this study, i.e. 50, 100, 200, and 300 ppm for GO and 500, 1000, 2000, and 3000 ppm for other DAIs. The SARA (Saturates, Aromatics, Resins and Asphaltenes) analysis of reservoir crude oil with ^{o}API of 23.65 was reported in Table 1. The colloidal instability index (CII) was considered to investigate the instability of the crude oil. It should be noted that the CII is an index which highlights the ratio of asphaltene and saturate summation to the summation of resins and aromatics. If the CII value of a crude oil sample is greater than 0.9, the crude oil is expressed as unstable (Ghloum et al., 2010 and 2019). However, according to SARA data, the CII value for reservoir crude oils is 1.60, and it demonstrates the asphaltene precipitation possibilities for these cases. However, in this work, the recombined live oil was used in the experiments to study the asphaltene deposition at the reservoir conditions. The results of a constant composition expansion (CCE) experiment were used to guarantee that the recombined oil could represent the in-situ reservoir fluid with acceptable accuracy. The CCE result illustrates that the measured bubble point pressure is

consistent with the real reservoir oil bubble point pressure (Gandomkar et al., 2012). The reservoir pressure and temperature are 3150 psia and 60 ^{o}C, respectively.

Table 1

- **Cloud point pressure measurements**

The authors considered liquid-free additives as DAIs throughout CO_2 injection at the reservoir conditions. The dissolution of DAIs (GO, TiO_2, SiO_2, and MgO) in CO_2 was investigated by calculation of cloud point pressures. The cloud point appears the pressure at which cloudiness in the solution is first observed as the pressure is lowered. It was measured by HPHT visual cell with different concentrations based on our previous work (Azizkhani and Gandomkar, 2020). At first, a determined amount of DAI is weighed out and insert into the window cell. After that, a specified amount of CO_2 was added to the sample to provide the desired composition. The mixture with constant total composition was pressurized and then used a magnetic stirrer to create a rotating magnetic field (2000 rpm). It was continued to achieve single-phase solutions from the window cell at favorable temperatures and pressures. Finally, the reduction in pressure of all samples was considered at the intervals of 40 psi. The equilibrium condition took about two hours to identify any visual changes. Also more time might be needed for the low solubility materials. In general, the cloud point pressures of DAI/CO_2 were indicated in the fog form by visual monitoring in the bulk sample (Miller et al., 2009; Lee et al., 2016). The measurements were repeated at least three times with reproducibility of ±5 psi. Subsequently, these mixtures were considered in all experiments to certify that the single-phase solution has occurred.

- **Minimum miscibility pressure (MMP)**

The IFT measurements between the live oil and DAI/CO_2 were performed by the high-pressure high-temperature IFT 700 apparatus. All the mixtures of hydrocarbon gas and DAIs were provided and then used to measure the IFTs at reservoir conditions (i.e. 3150 psia and 60 ^{o}C). An oil droplet is produced from the end of the capillary needle, which surrounded by pure CO_2 or DAI/CO_2 at required conditions. However, the IFTs were measured using advanced drop shape analysis software. In addition, the IFT error calculated via the standard deviation of 4 repeated measurements of each mix, and it was about ± 0.1. Also, the MMP measurement was conducted using vanishing interfacial tension (VIT) procedure (Azizkhani and Gandomkar, 2020; Ghorbani et al., 2014).

- **Asphaltene precipitation, Static test**

To investigate the asphaltene precipitation throughout the injection of CO_2 and CO_2/DAI, the PVT analysis was conducted. The PVT apparatus that was used in this study consisted the followings: PVT cell, transfer container, back pressure regulation, air bath, HPLC pump, sampling vessel, filter, recombination cell, and shaker. In the experiment, a certain volume of the CO_2/DAI mixture was injected into the PVT cell that contained live oil at the reservoir conditions. Next, the PVT cell was shaken for 24 hours at a chosen temperature and pressure. Then, the mixture of the CO_2/DAI and live oil was then retained in a stationary position for another day to ensure that the asphaltene precipitation was occurring. The crude oil sampling is taken out for analysis of asphaltene precipitation during CO_2/DAI injection. High-pressure filtration was used to separate the precipitated asphaltene from the oil at a constant pressure during its displacement from the PVT cell into the sampling vessel. Subsequently, the IP 143

standard method was conducted to measure the amount of the asphaltene content of the sample for all CO_2/DAI mixtures (Azizkhani and Gandomkar, 2020; Arciniegas et al., 2014).

- **Asphaltene deposition, Dynamic test**

In order to study the impact of DAIs on the asphaltene precipitation and its deposition, a series of coreflooding experiments were conducted during immiscible/miscible injection of CO_2. Full details of the coreflooding process, the core flood apparatus and its components are provided elsewhere (Gandomkar et al., 2015). To understand the impact of DAIs on asphaltene precipitation and its subsequent deposition, the miscible CO_2/DAIs was injected into carbonate core samples with the initial water and oil saturations similar to those of the initial reservoir conditions. In the course of the core flood experiments, the produced oil was gathered to measure the asphaltene deposition into the carbonate cores. To accurately determine the asphaltene content in the produced oil using spectrophotometry, a minimum of one gram of produced oil sample was required (Nguele et al., 2016; Srivastava et al., 1999; Li et al., 2018). The CO_2 injection was conducted up to two pore volumes with a frontal advance rate of 0.1 cm^3/min. Also, the scaling criterion of Rappaport and Leas (1953) has been considered to remove the dependence of oil recovery factor on core length and gas injection rate due to capillary end effect. It should be noted that the amount of asphaltene deposition was estimated by subtraction of the asphaltene content of the original crude oil from that of the produced oil. The amount of asphaltene deposition divided by initial asphaltene content and has been reported as a dimensionless parameter. The properties of carbonate cores were reported in Table 2. The average porosity and permeability ranged between 13 to 16 percent and 7 to 9 md, respectively (Cao et al., 2013).

Table 2

3. Results and discussion

The effect of GO, TiO_2, SiO_2, and MgO, as direct asphaltene inhibitors, on asphaltene precipitation and deposition was studied during miscible CO_2 injection. The SARA analysis and CII values were conducted to show the asphaltene precipitation possibilities for these cases. Besides, the cloud point pressure of all the CO_2/nanoparticles mixtures was measured to ensure that the single-phase conditions have occurred during asphaltene precipitation tests. Also, the asphaltene precipitation and deposition investigated by static and dynamic tests, respectively at reservoir conditions (i.e. 60 ^oC and 3150 psia).

- **Phase behavior of DAI/CO_2 by cloud point pressure measurements**

In Table 3, the cloud point pressures of CO_2 mixtures with GO, TiO_2, SiO_2, and MgO for different temperatures of 25, 40, 60, and 80 ^oC is listed. It should be noted that, throughout cloud point pressure measurements, the concentration of nano-particles were ranging from 50 to 300 ppm for GO and 500 to 3000 ppm for others. The cloud point pressures were ranging from 1400 to nearly 2500 psia. The cloud point pressure normally rises as the concentration of nano-particles in the solution increases. Additionally, the cloud point pressures increase almost linearly with increase in temperature. e.g., the cloud point pressures of GO illustrated that the dissolution of direct asphaltene inhibitor in CO_2 has occurred at 1712, 1830, 1994, and 2159 psia in different concentration; 50, 100, 200, and 300 ppm; respectively at reservoir temperature (i.e. 60 ^oC). According to these observations, all the cloud point pressures are lower than reservoir pressure and consequently, the single-phase conditions occur during asphaltene precipitation/deposition tests for all direct asphaltene inhibitors. The effect of temperature on the cloud point pressure of CO_2/DAI is shown in Figure 1 at different concentrations. Additionally, the solubility of DAIs increase as the temperature decreases. This observation highlights that the

density is directly proportional to the solubility. It could be explained by the entropy of mixing and its dependency to the temperature. The density of CO_2 reduces significantly at higher temperatures, whereas the impact of temperature on the nanoparticles density is minimal. If the density of CO_2 becomes significantly different from that of nanoparticles, the entropy of mixing becomes negative and then the temperature has a converse impact on the system (Joung et al., 2002). Based on these results, the cloud point pressures of GO are lower than other nanoparticles considered in this study at the same temperature. The molecular weights of nanoparticles have an impact on the solubility in CO_2, this is due to entropic impacts and coupled with the unwanted enthalpy interactions related to the CO_2-phobic functionalities and CO_2 (Yu et al., 2014; Chu et al., 2019). As it was observed, all the DAIs/CO_2 mixtures were single-phase at reservoir conditions and then these solutions were used for all asphaltene precipitation experiments.

Table 3

Figure 1

- **MMP measurements**

The amount of asphaltene precipitation will be different during miscible and immiscible CO_2 injection. Cao et al., (2013) illustrated that the miscible CO_2 injection causes more asphaltene precipitation compared to immiscible injection. However, in this study, vanishing interfacial tension technique was used to investigate the effect of DAI on MMP. At first, at equilibrium pressures ranging from 2500 to 3150 psia, the interfacial tension between live oil and pure/DAIs CO_2 were assessed. It should be noted that all the IFT values were measured at the reservoir temperature and pressures higher than the cloud point pressure to make sure that the mixtures of the CO_2/Nanoparticles are single phase. In Table 4, the results of live oil-pure CO_2 and

DAIs/CO_2 mixtures at T_{res}= 60 ^{o}C are listed. Considering the data of Table 4, the IFT for pure CO_2, 200 ppm GO, 2000 ppm TiO_2, 2000 ppm SiO_2, and 2000 ppm MgO are 46, 13, 15, 14, and 15 dyne/cm, respectively at 2500 psia and 60 ^{o}C. The asphaltenes are known to be one of the most surface-active compounds in crude oil and could be absorbed to the DAIs surface and reduce the IFTs. The metal oxide (DAIs) surface will typically have high surface energy. It was noted that GO could expressively decrease IFT compared to other DAIs considered in this study. It referred to the high specific surface area of GO compared to other DAIs. In addition, an increase in equilibrium pressure led to a significant reduction in IFT. It is well understood that as the IFT between live oil and nanoparticles/carbon dioxide decreases it will increase the miscibility and subsequently leads to a decrease in the residual oil saturation (Ghorbani et al., 2014). As shown in Figure 2, it is noted that MMP decreases as the concentration of the nanoparticles increases. It is due to the fact that the density of the mixture of the nanoparticles and CO_2 is slightly larger than the pure carbon-dioxide; this leads to a lower difference in density with that of the live oil and therefore smaller IFT values than pure carbon-dioxide (Chu et al., 2019). It is also shown that the MMP for GO/CO_2 is lower than that of the other mixtures. The MMPs are 3370, 2941, 3006, 2938, and 3040 psia for pure CO_2, 200 ppm GO, 2000 ppm TiO_2, 2000 ppm SiO_2, and 2000 ppm MgO, respectively at reservoir temperature, 60 ^{o}C. Hence, the MMP for pure CO_2 is above the P_{res}=3150 psi; and consequently, the immiscible conditions will occur during pure CO_2 injection for asphaltene precipitation/deposition tests. Furthermore, the MMPs for all CO_2/DAIs are smaller than reservoir pressure, and as a result, miscible conditions occur during static and dynamic asphaltene processes.

Table 4

Figure 2

- **PVT analysis of asphaltene precipitation through CO_2/DAI injection**

In this work, the team used nanoparticles as direct asphaltene inhibition agent to prevent the asphaltene precipitation by static test during CO_2 injection. In all experiments, to guarantee that all solutions are single-phase, the mixtures of CO_2/nanoparticles were injected at a pressure higher than the cloud point pressure. The live oil has 6.4 weight percent initial asphaltene content and from Table 5, the amounts of 5.8 weight percent asphaltene precipitated during pure immiscible injection of CO_2. It was expected that the amount of asphaltene precipitation increases during miscible DAIs/CO_2 but it reduced using nanoparticles as direct asphaltene inhibitors. The amount of asphaltene precipitation reduced from 5.8 to 3.1, 4.2, 4, and 3.8 weight percent by using 100 ppm GO, 1000 ppm TiO_2, 1000 SiO_2, and 1000 ppm MgO mixtures, respectively. Additionally, the CO_2/GO mixtures decreased the amounts of asphaltene precipitation higher than other DAIs considered in this study. The specific surface area of the GO (890 m^2/g) is higher than that for TiO_2 (174.5 m^2/g), SiO_2 (590 m^2/g), and MgO (300 m^2/g); consequently, it led to more adsorption of asphaltene (Yu et al., 2014; Karambeygi et al., 2016; Chu et al., 2019). The application of nanoparticles could enhance the solubility of asphaltene in the live oil and consequently lead to a reduction in the precipitation of asphaltene. Likewise, it increases the CO_2 solubility, dilutes the live oil, subsequently disperses the resin molecules, and finally leads to asphaltene stabilization in oil. Also, the amounts of asphaltene precipitation decreased by increasing DAI concentrations. The lone pair electrons, i.e., a pair of valence electrons, of oxygen intensify the surface negative charge density of the metal oxide nanoparticles, which enhances the adsorption of asphaltene fraction. It should be noted that there is an insignificant reduction in asphaltene precipitation for the duration of a high concentration of DAIs. For example, the amounts of asphaltene precipitation are 2.5 and 2.4 weight percent for

200 and 300 ppm GO, respectively. For that reason, the DAI concentration of 200 ppm can be more efficient than other DAI concentrations through miscible CO_2/GO injection. It was previously reported that the optimal concentration for Fe_3O_4 and TiO_2 nanoparticles in the inhibitor is approximately one weight percent (Hassanpour et al., 2018). In addition, it will decrease the asphaltene precipitation to seventeen and eighteen percent of initial content of asphaltene using TiO_2 and Fe_3O_4 correspondingly. When a low concentration of inhibitor is applied, active site on the structure of asphaltene could be occupied by free monomers and consequently stabilizes the asphaltene particles within the solution (Rocha et al., 2006). Additionally, the polar head group of the inhibitor has a dissimilar potential to attach to the particles and makes the system of the inhibitor/asphaltene more stable. It should be highlighted that these groups' polarity governs the strength of the bond. However, when a high concentration of inhibitors is used, it will not lead to the desired result. As the inhibitors' concentration rises, the likelihood of self-association under hydrogenous bonding increases accordingly. Conversely, when a higher concentration of inhibitor is applied, the potential of self-association in inhibitor-inhibitor is larger than the inhibitor/asphaltene's interaction. Consequently, the capability of inhibitors on the stabilization of the asphaltenes decreases and it will cause the inhibitors to underperform at higher concentrations (Karambeygi, 2016; Leon et al., 2001). As a result, the metal oxide nanoparticles have acidic/basic/amphoteric chemical characteristic, which causes polar interactions between asphaltenes particles and nanoparticles. The bond formation between nanoparticles (metal oxide) and asphaltene particles is a key factor that delays the beginning point of separation of asphaltenes from oil, i.e., onset. The asphaltene particles could be suspended in resins due to the formation bonding of metal-oxide nanoparticles and asphaltene molecules and its bonding to the activated sites on the surface of the asphaltene particles (Nassar

et al., 2011). It should be noted there are two conflicting forces affecting the precipitation, i.e., aggregation effect and the solubility mechanism. The first force (aggregation effect) has a tendency to lead to precipitation whilst the second (solubility mechanism) tends to retain the asphaltene molecules in the solution. Furthermore, the results show that the impact of the solubility mechanism is more dominant than that of the aggregation effect for the duration of the injection of CO_2/nanoparticles (Gharbi et al., 2017; Rashid et al., 2019; Yen et al., 2001).

Table 5

- **The effect of DAI on asphaltene deposition**

The amount of asphaltene deposition into the carbonate cores was measured during coreflooding tests for pure and CO_2/DAIs injection. Figure 3 shows the variation in the asphaltene content of the produced oil with injected PV of pure and CO_2/DAIs injection during carbonate cores. The asphaltene concentration in the oil was constant till CO_2 breakthrough which occurred at around 0.25 pore volumes (PV) and 0.35 PV for pure CO_2 and CO_2/DAIs mixtures, respectively. Because the produced oil had not yet been in contact with the injected pure CO_2 and CO_2/DAIs, the change in asphaltene content was insignificant. Inversely, the asphaltene content in the produced oil after the CO_2 breakthrough reduced significantly. The drop in asphaltene content highlights the fact that some further asphaltene precipitation/flocculation occurs in the carbonate cores during pure and CO_2/DAIs injection. From Figure 3, the asphaltene content in produced oil during injection of DAIs/CO_2 mixtures are higher than that for pure CO_2 injection. It shows that the metal oxide nanoparticles can stabilize the asphaltene particles in reservoir oil. In addition, the mixture of GO/CO_2 improved the asphaltene stabilization compared to other DAIs considered in this study. From this result, the amount of asphaltene content in produced oil are 1.3, 5.4, 4.1, 3, and 5 weight percent after injection of 2 PV pure CO_2, 200 ppm GO, 2000 ppm

SiO_2, 2000 TiO_2, and 2000 ppm MgO mixtures, respectively. Also, Figure 4 illustrates the amount of asphaltene's deposition in the carbonate cores by the subtraction of the asphaltene content in the produced oil from that of the initial crude oil during the dynamic tests. The amount of asphaltene deposition significantly decreased during injection of CO_2/DAIs mixtures compared to pure CO_2 injection. The metal oxide nanoparticles hinder the phase separation of asphaltenes kinetically and prevent growth. It is conducted by stabilizing the colloidal suspension of the asphaltene particles, which are in sub-micrometer size to significantly slow the asphaltene flocculation onset. Consequently, the direct asphaltene inhibitors can prevent to asphaltene deposition and act as asphaltene dispersants. The polyaromatic nuclei with aliphatic side chains and rings of asphaltene connect and create micellar aggregates. This is well-documented that in addition to aromatic compounds, asphaltenes consist of different acidic and basic functional groups. The metal oxide nanoparticles that are adsorbed on the micelle core make the asphaltene micelles more stable. The DAIs connects to the asphaltene particles using their polar head and expands their aliphatic group outward. This creates a layer round asphaltenes. On the condition that the asphaltene particles are stabilized in the micelles, precipitation does not occur (Setaro rt al., 2019).

Figure 3

Figure 4

Besides, using asphaltene particle size analysis approach, the team measured the mean size of the asphaltene particles to study the impact of direct asphaltene inhibitors on asphaltene particle size for the duration of pure CO_2 injection and 200 ppm GO/CO_2 mixture injection, Figures 5 and 6. Based on this result, the asphaltene particle size during pure CO_2 injection is higher than that for GO/CO_2 mixture injection. It is clear that the GO/CO_2 mixtures can stabilize the asphaltene

particles in oil and significantly reduces the size of asphaltene particles simultaneously. The total size of asphaltene particles which precipitated during the injection of pure CO_2 and 200 ppm GO/CO_2 mixture are 2657808 and 756592 μm^2, respectively. The particles are created in two different stages, i.e., phase separation stage and asphaltene particle growth stage. Phase separation takes place when asphaltene particles in the oil precipitate and develop into large aggregates. Additionally, the stability of asphaltene particles can be improved by the introduction of compounds, which hold a polar head containing an acidic group, which can attach to the micellar core. Dissimilar acidities are observed for amphiphiles with diverse head groups. The inhibition capability of amphiphiles depends on the fact that how strong are their groups' acidity, therefore the amphiphiles stabilize the asphaltene in the solution via the acid-base interaction. The ability of amphiphiles' inhibition is related to the strength of these groups acidity and illustrating that the asphaltene stabilization occurs through the acid-base interaction (Zanganeh et al., 2018). However, direct asphaltene inhibitors can decrease the amount of asphaltene precipitation and also prevents the aggregation of precipitated asphaltene particles. By the way, the size of deposited asphaltene particles can affect the oil flow in porous media due to changing the pressure drop. Based on the dynamic tests, the differential pressure during the pure CO_2 injection was higher than that for injection of CO_2/DAIs mixtures. It referred to asphaltene precipitation, which increased formation damage during the pure CO_2 injection compared to other cases. Figure 7 shows the schematic of asphaltene deposition on the rock surface. The asphaltenes may adsorb onto the rock surface and cause permeability blockage, wettability alteration to oil-wet, reduces the oil effective permeability; and thereby decreases the oil recovery (Figure 7a). However, the application of direct asphaltene inhibitors can stabilize the asphaltene particles and also prevent to asphaltene deposition as a dispersant (Figure 7b).

Additionally, the presence of the metal oxide nanoparticles as direct asphaltene inhibitors can enhance the oil recovery factor between 6 to 25 percent compared to pure CO_2 injection. The adsorption performance of asphaltenes on the metal oxide nanoparticles is governed by two properties, i.e., the surface energy and the structure of nanoparticles and the chemical and physical characteristics of the asphaltene particles and polar, electrostatic, and van der Waals interactions are the key factors which influence the asphaltene adsorption onto the solid surfaces. Among these three factors, the acid−base (polar) and electrostatic interaction are the most significant factors. It is well-documented that surface Gibbs energy reduced by the adsorption of asphaltene particles on the nanoparticles. Consequently, the nanoparticles containing asphaltene (which are adsorbed onto the surface of nanoparticles) have a weaker interaction compared to those of the nanoparticles lacking asphaltene particles. Hence, the adsorbed asphaltene particles onto the nanoparticles have higher stability in the reservoir rock (Hosseinpour et al., 2013; Castro et al., 2009). Throughout the CO_2/DAIs injection, the nanoparticles adsorb the precipitated asphaltene particles and consequently alleviate the rate of the adsorption of precipitated asphaltenes onto the rock surface and consequent deposition in the porous medium. For that reason, the nanoparticles carrying asphaltenes could travel within the porous medium and subsequently lead to inhibit the precipitation and as a result, prevents permeability reduction due to asphaltene precipitation.

Figure 5

Figure 6

Figure 7

4. Conclusions

- Liquid-free inhibitors can be directly applicable for gas-based enhanced oil recovery in field scale.
- The metal oxide nanoparticles could increase the stability of the colloidal asphaltenes and consequently diminish the growing and the formation of flocculated asphaltene particles.
- The total size of asphaltene particles, which precipitated during injection CO_2/DAIs mixture, is significantly lower than that for pure CO_2 injection.
- The effectiveness of the graphene oxide nanoparticle is much better than other DAIs in retaining the asphaltene particles suspended and spread within the oil.
- The application of CO_2/GO mixtures could reduce the asphaltene aggregation/deposition and improved the oil recovery factor between 6 to 25 percent compared to the case that only CO_2 was injected.
- The cloud point pressure of CO_2/DAIs mixtures is under the reservoir pressure to certify that the single-phase solution has occurred at reservoir conditions.
- The direct asphaltene inhibitors lead to a decrease in the IFT and provide the miscible injection of gas at reservoir pressure and temperature.
- The metal oxide nanoparticles improved the solubility of the asphaltene particles and consequently kept them in the solution.

Nomenclature

Colloidal Instability Index, CII

Constant Composition Expansion, CCE

Cubic Plus Association Equation of state, CPA

Deasphalted Crude Oil, DO

Direct Asphaltene Inhibitor, DAI

Dodecyl Benzene Sulfonic Acid, DDBSA

Dodecyl Risolsinol, DR

Graphene Oxide, GO

High-Pressure High-Temperature, HPHT

Liquefied Petroleum Gas, LPG

Magnesium Oxide, MgO

Minimum Miscibility Pressure, MMP

Nonyl Phenol, NP

Pressure, Volume, Temperature, PVT

Resins, R

Saturates, Aromatics, Resins, and Asphaltenes, SARA

Silicon Dioxide, SiO_2

Titanium Dioxide, TiO_2

Toluene, T

Vanishing Interfacial Tension, VIT

Weight percent, wt

References

Arciniegas, L.M., Babadagli, T., Asphaltene precipitation, flocculation and deposition during solvent injection at elevated temperatures for heavy oil recovery, Fuel Journal, 124, 202-211, 2014.

Azizkhani A., Gandomkar, A., A novel method for application of nanoparticles as direct asphaltene inhibitors during miscible CO_2 injection, Journal of Petroleum Science and Engineering, 185, 106661, 2020.

Bae, J., Fouchard, D., Garner, S., Macias, J., Advantages of Applying a Multifaceted Approach to Asphaltene Inhibitor Selection, OTC 27171, 2016.

Cao, M., Gu, Y., Oil recovery mechanisms and asphaltene precipitation phenomenon in immiscible and miscible CO_2 flooding processes, Fuel Journal, 109, 157-166, 2013.

Castro, M., Cruz, J.L., Ramirez, S., Villegas, A., Predicting adsorption isotherms of asphaltenes in porous materials, Fluid Phase Equilibria, 286, 113-119, 2009.

Chu, T.M., Nguyen, N.T., Vu, T.L., Pham, T.D., Synthesis, Characterization, and Modification of Alumina Nanoparticles for Cationic Dye Removal, Materials, 12, 450, 1-15, 2019.

Dai, J.F., Wang, G.J., Wu, Ch., Investigation of the Surface Properties of Graphene Oxide and Graphene by Inverse Gas Chromatography, Chromatographia journal, 77, 299-307, 2014.

Gandomkar, A., Kharrat, R., Tertiary FAWAG Process on Gas and Water Invaded Zones, an Experimental Study, Journal of Energy Sources, Part A: Recovery, Utilization, and Environmental Effects, 34, 1913-1922, 2012.

Gandomkar, A., Rahimpour, M.R., Investigation of low salinity waterflooding in secondary and tertiary enhanced oil recovery in limestone reservoirs, Energy & Fuels Journal, 29, 7781-7792, 2015.

Gharbi, Kh., Benyounes, Kh., Khodja, M., Removal and prevention of asphaltene deposition during oil production: A literature review, Journal of Petroleum Science and Engineering, 158, 351-360, 2017.

Ghloum, E.F., Qahtani, M.A., Rashid, A., Effect of inhibitors on asphaltene precipitation for Marrat Kuwaiti reservoirs, Journal of Petroleum Science and Engineering, 70, 99-106, 2010.

Ghloum, E.F., Rashed, A.M., Safa, M.A., Mitigation of asphaltenes precipitation phenomenon via chemical inhibitors, Journal of Petroleum Science and Engineering, 175, 495-507, 2019.

Ghorbani, M., Momeni, ., Safavi, S., Gandomkar, A., Modified Vanishing Interfacial Tension (VIT) Test for CO_2-Oil Minimum Miscibility Pressure (MMP) Measurement, Journal of Natural Gas Science and Engineering, 20, 92-98, 2014.

Hassanpour, S., Malayeri, M.R., Riazi, M., Utilization of CO_3O_4 nanoparticles for reducing precipitation of asphaltene during CO_2 injection, Journal of Natural Gas Science and Engineering, 31, 39-47, 2016.

Hassanpour, S., Malayeri, M.R., Riazi, M., Asphaltene Precipitation during Injection of CO_2 Gas into a Synthetic Oil in the Presence of Fe_3O_4 and TiO_2 Nanoparticles, Journal of chemical engineering data, 63 (5), 1266-1274, 2018.

Hong, E., Watkinson, P., A study of asphaltene solubility and precipitation. Fuel journal, 83, 1881-1887, 2004.

Hosseinpour, N., Khodadadi, A.A., Bahramian, A., Mortazavi, Y., Asphaltene adsorption onto acidic/basic metal oxide nanoparticles toward in situ upgrading of reservoir oils by nanotechnology, Langmuir, 29, 14135-14146, 2013.

Hu, Y.F., Guo, T.M., Effect of the structures of ionic liquids and alkylbenzenederived amphiphiles on the inhibition of asphaltene precipitation from CO_2-injected reservoir oils, Langmuir, 21, 8168-8174, 2005.

Ibrahim, H.H., Idem, R.O., Inter relationships between Asphaltene Precipitation Inhibitor Effectiveness, Asphaltenes Characteristics, and Precipitation Behavior during n-Heptane (Light Paraffin Hydrocarbon) -Induced Asphaltene Precipitation, Energy & Fuels, 18, 1038-1048, 2004.

Joonaki, E., Burgass, R., Hassanpouryouzband, A., Tohidi, B., Comparison of experimental techniques for evaluation of chemistries against asphaltene aggregation and deposition: new application of high-pressure and high-temperature quartz, Energy & Fuels, 32, 3, 2712-2721, 2017.

Joonaki, E., Buckman, J., Burgass, R., Tohidi, B., Water versus Asphaltenes; Liquid–Liquid and Solid–Liquid Molecular Interactions Unravel the Mechanisms behind an Improved Oil Recovery Methodology, Scientific Reports, 9, 1, 11369, 2019.

Joonaki, E., Hassanpouryouzband, A., Burgass, R., Hase, A., Tohidi, B., Effects of Waxes and the Related Chemicals on Asphaltene Aggregation and Deposition Phenomena: Experimental and Modeling Studies, ACS omega 5, 13, 7124-7134, 2020.

Joung, S.N., Park, J.U., Kim, S.Y., High-pressure phase behavior of polymersolvent systems with addition of supercritical CO_2 at temperatures from 323.15 K to 503.15 K, Journal of Chemical & Engineering Data, 47, 2, 270-273, 2002.

Karambeygi, M.A., Nikazar, M., Kharrat, R., Experimental evaluation of asphaltene inhibitors selection for standard and reservoir conditions, Journal of Petroleum Science and Engineering, 13, 74-86, 2016.

Kazemzadeh, Y., Malayeri, M.R., Riazi, M., Parsaei, R., Impact of Fe_3O_4 nanoparticles on asphaltene precipitation during CO_2 injection, Journal of Natural Gas Science and Engineering, 22, 227-234, 2015.

Kelland, M.A., Asphaltene control. Production Chemicals for the Oil and Gas Industry. Stavanger, Norway: University of Stavanger, Chapter 4, 2009.

Leonard, G.Ch., Ponnapati, R., Rivers, G., Novel Asphaltene Inhibitor for Direct Application to Reservoir, SPE 167294, 2013.

Leon, O., Contreras, E., Rogel, E., Dambakli, G., Espidel, J., Aevedo, S., The influence of the adsorption of amphiphiles and resins in controlling asphaltene flocculation, Energy and Fuels, 15, 102-1032, 2001.

Lee, J.J., Dhuwe, A., Stephen, D., Eric, J., Enick, R.M., Polymeric and Small Molecule Thickeners for CO_2, Ethane, Propane and Butane for Improved Mobility Control, SPE Improved Oil Recovery Conference, Tulsa, SPE 179587, 2016.

Li, X., Guo, Y., Sun, Q., Lan, W., Guo, X., Experimental study for the impacts of flow rate and concentration of asphaltene precipitant on dynamic asphaltene deposition in microcapillary medium, Journal of Petroleum Science and Engineering, 162, 333-340, 2018.

Lu, T., Li, Zh., Fan, W., Zhang, X., Nanoparticles for Inhibition of Asphaltenes Deposition during CO_2 Flooding, Industrial & Engineering Chemistry Research, 55 (23), 6723-6733, 2016.

Miller, M.B., Chen, D.L., Xie, H.B., Luebke, D.R., Enick, R.M., Solubility of CO_2 in CO_2-philic oligomers; cosmotherm predictions and experimental results, fluid phase equilibria, 287, 26-32, 2009.

Nassar, N.N., Hassan, A., Pereira, A.P., Metal oxide nanoparticles for asphaltene adsorption and oxidation, Energy & Fuels, 25, 3, 1017-1023, 2011.

Nguele, R., Ghulami, M.R., Sasaki, K., Asphaltene Aggregation in Crude Oils during Supercritical Gas Injection, Energy and Fuels, 30, 2, 1266-1278, 2016.

Rappaport, L.A., Leas, W.J. 1953," Properties of Linear Waterfloods, presented at the Fall Meeting of the Petroleum Branch in Houston, Texas, SPE 213-G.

Rashid, Z., Wilfred, C.D., Murugesan, Th., A comprehensive review on the recent advances on the petroleum asphaltene aggregation, Journal of Petroleum Science and Engineering, 176, 249-268, 2019.

Reubush, S. D., Effects of storage on the linear viscoelastic response of polymer-modified asphalt at intermediate to high temperatures, MS Thesis, Virginia Polytechnic Institute and State University, Blacksburg, VA, 1999.

Rocha, L.C., Ferreira, M.S., Ramos, A.C., Inhibition of asphaltene precipitation in Brazilian crude oils using new oil soluble amphiphiles, Journal of Petroleum Science and Engineering, 51, 26-36, 2006.

Setaro, L.O., Pereira, V.J., Costa, G.M., Melo, S., A novel method to predict the risk of asphaltene precipitation due to CO_2 displacement in oil reservoirs, Journal of Petroleum Science and Engineering, 176, 1008-1017, 2019.

Shojaati, F., Riazi, M., Mousavi, S.H., Experimental investigation of the inhibitory behavior of metal oxides nanoparticles on asphaltene precipitation, Colloids and Surfaces A: Physicochemical and Engineering Aspects, 531, 99-110, 2017.

Srivastava, R.K., Huang, S.S., Dong, M., Asphaltene Deposition During CO_2 Flooding, SPE Production & Facilities, SPE 59092, 14, 4, 1999.

Stephenson, W.K., Producing Asphaltene Crude Oils: Problems and Solutions, Petroleum Engineer, 24, 1990.

Taher, A.S., Mohammed, A.F., Amal, S.E., Retardation of asphaltene precipitation by addition of toluene, resins, deasphalted oil and surfactants, Fluid Phase Equilibria 194-197, 1045-1057, 2002.

Varamesh, A., Hosseinpour, N., Prediction of Asphaltene Precipitation in Reservoir Model Oils in the Presence of Fe3O4 and NiO Nanoparticles by Cubic Plus Association Equation of State, Industrial & Engineering Chemistry Research, 58 (10), 4293-4302, 2019.

Yen, A., Yin, Y.R., Asomaning, S., Evaluating Asphaltene Inhibitors: Laboratory Tests and Field Studies, SPE 65376, 2001.

Yin, Y.R., Yen, A.T., Asphaltene Deposition and Chemical Control in CO_2 Floods, SPE-59293, 2000.

Yu, H., Li, Y., Fan, L., Yang, Sh., Highly dispersible and charge-tunable magnetic Fe_3O_4 nanoparticles: facile fabrication and reversible binding to GO for efficient removal of dye pollutants, Journal of Materials Chemistry A, 38, 2, 15763-15767, 2014.

Zanganeh, P., Dashti, .H, Ayatollahi, Sh., Comparing the effects of CH_4, CO_2, and N_2 injection on asphaltene precipitation and deposition at reservoir condition: A visual and modeling study, Fuel, 217, 633-641, 2018.

List of Tables

Table 1

Reservoir oil properties	Values
Saturates	55.10 wt
Aromatics	22.90 wt
Resins	15.60 wt
Asphaltenes	6.40 wt
CII	1.60
API	23.65
Molecular weight, g/mol, IP-86	164.80
S.G (60°F), ASTM-D40452	0.91
Acid Number, mg/g (KOH)	1.45
T_{res} (^{o}C)	60
P_{res} (psia)	3150

Table 2

Limestone Cores No.	Length (cm)	Diameter (in)	PV (cc)	Helium Porosity (Percent)	Permeability (mD)	Connate Water (Percent)
C1	7.5	1.5	11.9	13.91	7.5	27.9
C2	7.4	1.5	12.5	14.81	8.2	29.5
C3	7.7	1.5	13.3	15.15	8.6	28.4
C4	7.8	1.5	13.0	14.61	7.8	29.1
C5	7.7	1.5	13.1	14.92	8.3	28.5

Table 3

DAI	Concentration (ppm)	Cloud point pressure (psia)			
		25 °C	40 °C	60 °C	80 °C
GO	50	1419	1538	1712	1935
	100	1527	1659	1830	2061
	200	1670	1812	1994	2215
	300	1746	1971	2159	2406
TiO_2	500	1631	1724	1921	2126
	1000	1731	1862	2026	2243
	2000	1865	2028	2183	2388
	3000	1953	2159	2340	2589
SiO_2	500	1574	1663	1859	2080
	1000	1653	1725	1938	2180
	2000	1785	1947	2105	2300
	3000	1883	2082	2265	2497
MgO	500	1469	1575	1755	1971
	1000	1579	1690	1884	2118
	2000	1720	1882	2058	2263
	3000	1792	2046	2217	2483

Table 4

DAI	Concentration (ppm)	IFT (dyn/cm) Live oil/CO_2-DAI, T_{res}= 60 ^oC				
		P=2500 psia	P=2800 psia	P=3000 psia	P_{res} =3150 psia	MMP (psia)
GO	Pure CO_2	46	31	20	12	3370
	50	28	16	7	0	3100
	100	18	9	1	0	3049
	200	13	4	0	0	2941
	300	6	0	0	0	2740
TiO_2	500	34	19	8	0	3140
	1000	22	11	3	0	3115
	2000	15	6	1	0	3006
	3000	9	1	0	0	2811
SiO_2	500	31	16	5	0	3115
	1000	20	10	1	0	3027
	2000	14	4	0	0	2938
	3000	7	0	0	0	2761
MgO	500	30	19	8	0	3110
	1000	19	11	2	0	3100
	2000	15	7	0	0	3040
	3000	8	1	0	0	2814

Table 5

DAI	**Concentration (ppm)**	**Asphaltene Precipitation, Static Test** (wt%)
Pure CO_2		5.8
GO	50	4.0
	100	3.1
	200	2.5
	300	2.4
TiO_2	500	5.0
	1000	4.2
	2000	3.8
	3000	3.7
SiO_2	500	4.8
	1000	4.0
	2000	3.5
	3000	3.4
MgO	500	4.5
	1000	3.8
	2000	3.5
	3000	3.5

List of Figures

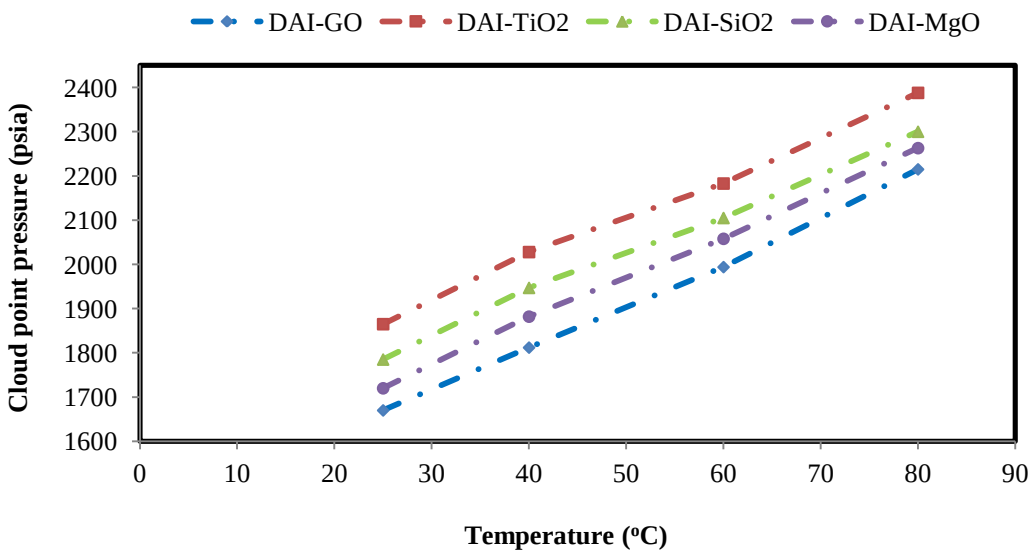
DAI-GO
DAI-TiO2
DAI-SiO2
DAI-MgO
Cloud point pressure (psia)
2400
2300
2200
2100
2000
1900
1800
1700
1600
0
10
20
30
40
50
60
70
80
90
Temperature (ºC)

Figure 1

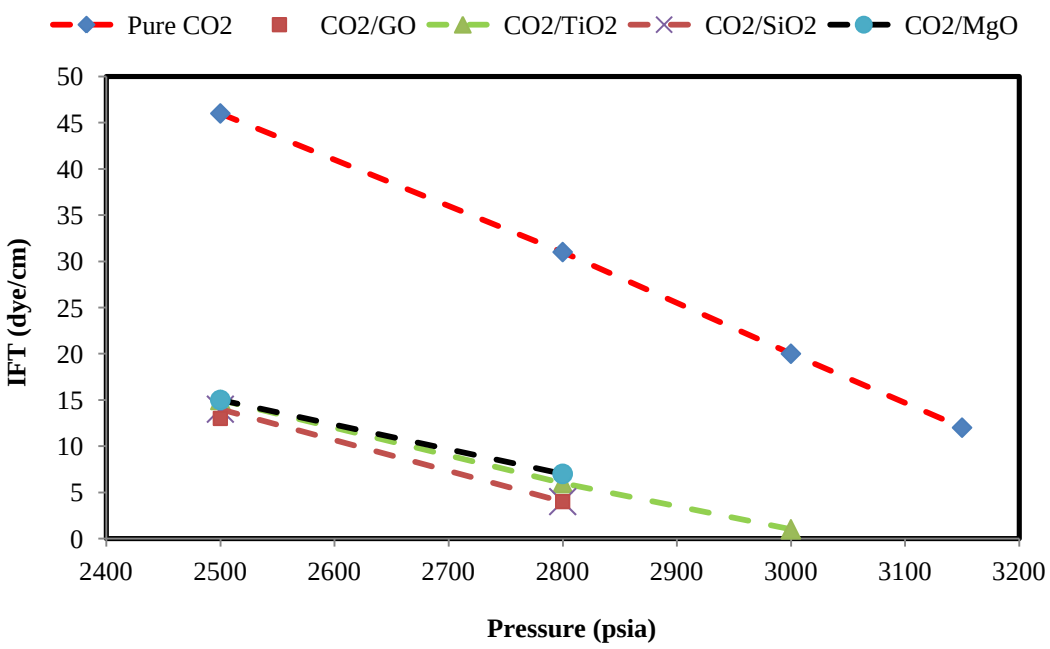
Pure CO2
CO2/GO
CO2/TiO2
CO2/SiO2
CO2/MgO
IFT (dye/cm)
50
45
40
35
30
25
20
15
10
5
0
2400
2500
2600
2700
2800
2900
3000
3100
3200
Pressure (psia)

Figure 2

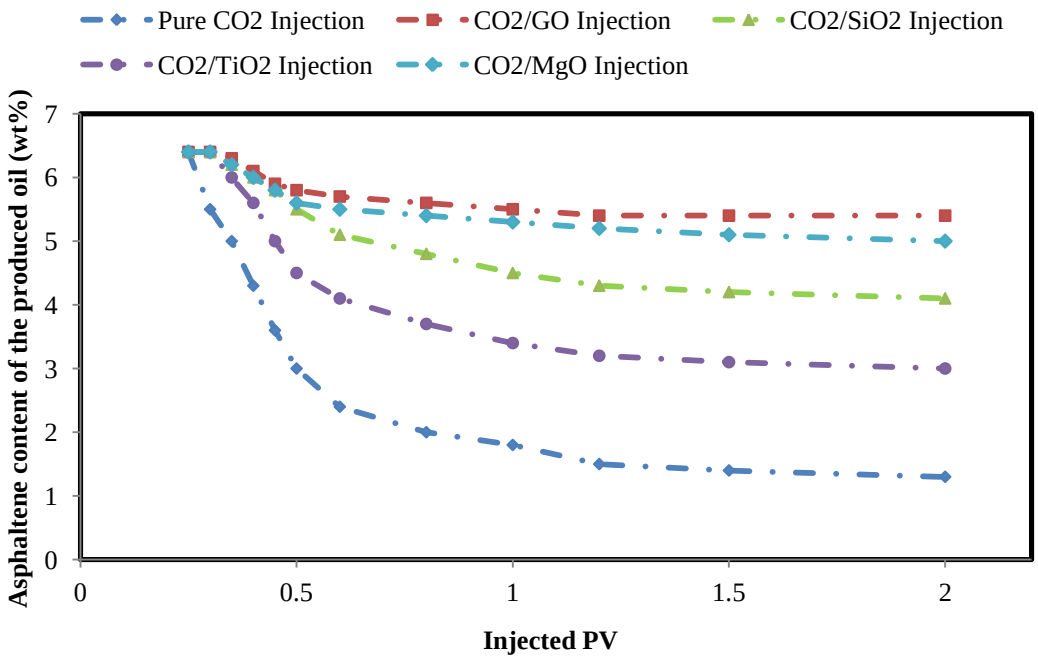
Pure CO2 Injection
CO2/GO Injection
CO2/SiO2 Injection
CO2/TiO2 Injection
CO2/MgO Injection
Asphaltene content of the produced oil (wt%)
0
1
2
3
4
5
6
7
0
0.5
1
1.5
2
Injected PV

Figure 3

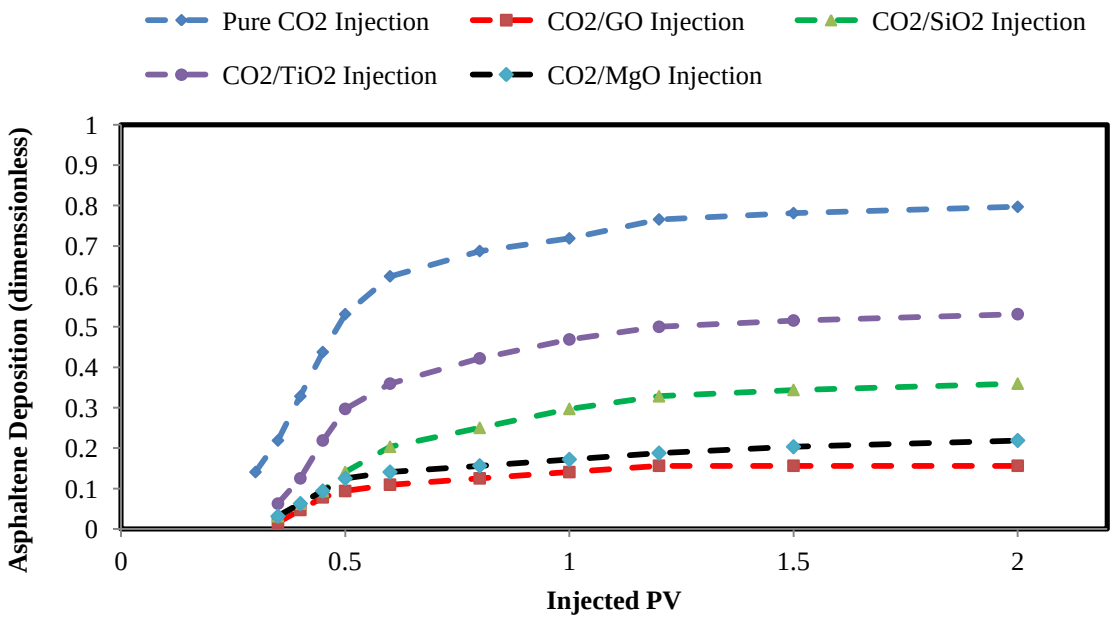
Pure CO2 Injection
CO2/GO Injection
CO2/SiO2 Injection
CO2/TiO2 Injection
CO2/MgO Injection
Asphaltene Deposition (dimenssionless)
Injected PV
0
0.1
0.2
0.3
0.4
0.5
0.6
0.7
0.8
0.9
1
0
0.5
1
1.5
2

Figure 4

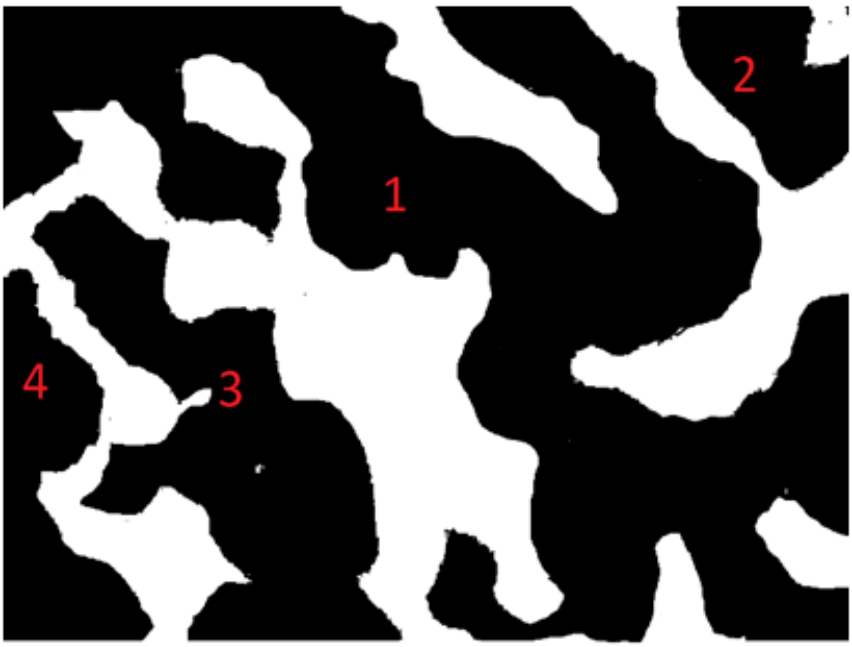

Particle number	1	2	3	4
Area (μm²)	1741670	157860	534393	223885
Total area (μm²)	2657808			

Figure 5

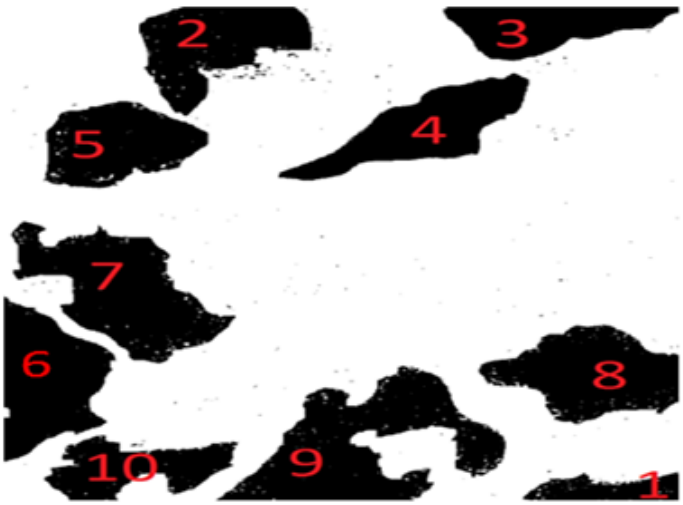

Particle number	1	2	3	4	5	6	7	8	9	10
Area (μm²)	29798	74005	53573	73264	68014	102846	104938	75591	125733	48830
Total area (μm²)	756592									

Figure 6

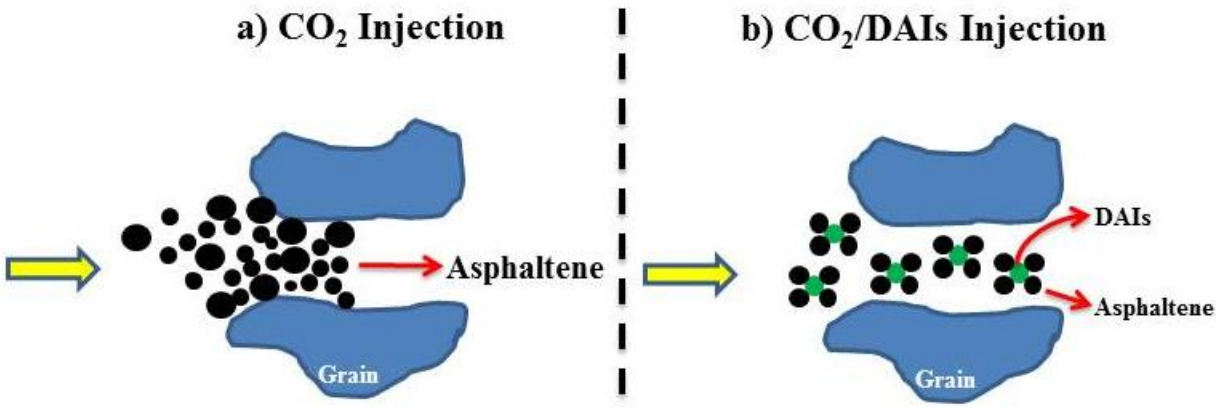
a) CO_2 Injection
b) CO_2/DAIs Injection
Asphaltene
Grain
DAIs
Asphaltene
Grain

Figure 7

***Declaration of Interest Statement**

Declaration of interests

☒ The authors declare that they have no known competing financial interests or personal relationships that could have appeared to influence the work reported in this paper.

☐The authors declare the following financial interests/personal relationships which may be considered as potential competing interests:

Credit author statement

Asghar Gandomkar: Conceptualization, Methodology, Validation, Investigation, Resources, Writing - Original Draft, Writing - Review & Editing, Visualization, Supervision, Project administration. **Hamid Reza Nasriani:** Methodology, Investigation, Writing - Original Draft, Writing - Review & Editing.